CNWRA®
A center of excellence in earth sciences and engineering®

Geosciences and Engineering Division
6220 Culebra Road • San Antonio, Texas, U.S.A. 78238-5166
(210) 522-5160 • Fax (210) 522-5155

September 25, 2015
Contract No. NRC–HQ–12–C–02–0089
Task Order 4
Account No. 20.17860.04

U.S. Nuclear Regulatory Commission
ATTN: Mr. Maurice Heath
Office of Nuclear Material Safety and Safeguards
Mail Stop TWFN 8F8
Washington, DC 20555

Subject: Intermediate Milestone 17860.04.004.510: Feasibility Study of Acoustic Emission Monitoring for Cracking of Waste-Stabilizing Tank Grout and Saltstone—A Progress Report

Dear Mr. Heath:

This letter transmits the subject intermediate milestone, prepared by the Center for Nuclear Waste Regulatory Analyses staff as part of the task order titled Technical Assistance for the Review of the U.S. Department of Energy's (DOE's) Non-High-Level Waste Determinations. Note that the title has been changed from "Tank Grout Acoustic Emission Method Development—Status Report" to more fully reflect the content. This report documents fiscal year 2015 activities to test the feasibility of using acoustic emission (AE) technology for monitoring crack formation within tank grout and saltstone, including during the early stages of hydration when the cementitious materials are in a gel form, difficult to monitor acoustically, and yet still susceptible to cracking. Cracks form preferential pathways through grout monoliths that enable rapid infiltration of meteoric water, which may suppress the chemically reducing effect of the grout. Using AE monitoring, it may be possible to record the timing and location of cracking and to map crack propagation. Such data might be used to improve understanding of the mechanisms of crack development and distribution of cracks. The work this fiscal year consisted of (i) ultrasonic through-transmission measurements of longitudinal and shear wave speeds and signal attenuation in hardened tank grout and saltstone specimens to define preliminary AE acquisition settings, (ii) AE sensor configuration definition and refinement, (iii) a 32-day AE monitoring experiment using a mesoscale specimen of hydrating tank grout, and (iv) a 3-day automated through-transmission experiment using bench-scale specimens of hydrating tank grout. Results indicate that two frequency bands are conducive to AE monitoring—one in the 100–150 kHz range and a second near 50 kHz. To optimize the AE monitoring technique, additional testing is planned in the next fiscal year to complete the characterization of the ultrasonic properties of tank grout and saltstone. If AE-based crack detection and location is proven successful at the mesoscale, then the monitoring approach may be further refined for potential implementation on actual waste tanks and saltstone vaults

Washington Office
1801 Rockville Pike, Suite 105 • Rockville, Maryland 20852-1633

for detecting cracks that may affect the capability of the cementitious grouts to provide low permeability reducing environments that limit release of key radionuclides.

The report is attached in PDF format. We also will make a Microsoft® Word® version of the report available to the U.S. Nuclear Regulatory Commission staff in a convenient location on the CNWRA-hosted shared drive.

If you have any questions regarding this report, please contact Dr. Cynthia Dinwiddie at (210) 522-6085 or me at (210) 522-5582.

Sincerely,

David Pickett

David Pickett, Ph.D., P.G.
Senior Program Manager
Transportation, Storage, Disposal and
Fuel Cycle Facilities

DP/lg
Enclosure
SHAREPOINT: DOE Non-High Level Waste Determinations 17860.04\Fiscal Year 2015

cc:

NRC	GED/CNWRA
Sharlene McCubbin	GED Correspondence
Harry Felsher	W. Patrick
Cynthia Barr	
Chris McKenney	
M. Lombard	
A. Hsia	
C. Schum	

Feasibility Study of Acoustic Emission Monitoring for Cracking of Waste-Stabilizing Tank Grout and Saltstone

A Progress Report

Prepared for

U.S. Nuclear Regulatory Commission
Contract No. NRC–HQ–12–C–02–0089

Prepared by

Alan R. Puchot
Adam C. Cobb
Cynthia L. Dinwiddie
Donald M. Hooper

Center for Nuclear Waste Regulatory Analyses
Southwest Research Institute®
San Antonio, Texas

September 2015

PREVIOUS REPORTS IN SERIES

Number	Name	Date Issued
14003.01.007.222	Conceptual Design for Small-Scale Grout Monolith Tests	April 2008
14003.01.007.305	Mesoscale Grout Monolith Experiments: Results and Recommendations	May 2009
14003.01.007.445	Intermediate-Scale Grout Monolith and Additional Mesoscale Grout Monolith Experiments: Results and Recommendations—Status Report	September 2010
14003.01.007.121	Bonding and Cracking Behavior and Related Properties of Cementitious Grout in an Intermediate-Scale Grout Monolith	September 2011
14003.01.007.122	Fiscal Year 2012 Meso- and Intermediate-Scale Grout Monolith Test Bed Experiments: Results and Recommendations (Final Report)	August 2012

CONTENTS

FIGURES

TABLES

EXECUTIVE SUMMARY

Large steel tanks are used to store liquid waste from processing nuclear materials as part of the defense programs of the U.S. Department of Energy (DOE). At the Savannah River Site (SRS), DOE has implemented a program to remove highly radioactive radionuclides from the tanks to the maximum extent practical and stabilize the residual waste inside the tanks using a cementitious chemically reducing grout. The purposes of the grout are to fill and structurally stabilize the tanks, and to provide a hydrologic and chemical barrier limiting the release of key radionuclides to the environment. Radionuclides that are removed from the tanks are encapsulated in another cementitious material known as saltstone, which is then permanently placed into underground vaults located at the SRS. The U.S. Nuclear Regulatory Commission (NRC) previously sponsored studies at the Center for Nuclear Waste Regulatory Analyses (CNWRA®) to better understand the potential for cracks and other preferential pathways to form in tank grout monoliths during the early years after grout is placed. Results from this study indicated that grout monoliths may be at risk for multiple cracking regimes, particularly in the first 24 hours post-placement.

The CNWRA is now providing technical assistance to the NRC to test the feasibility of acoustic emission (AE) technology for passively monitoring crack formation within cementitious tank grout and saltstone, including monitoring during the early stages of hydration when the cementitious materials are in a gel form and difficult to monitor acoustically. Using AE monitoring, it may be possible to record the timing and location of cracking and to map crack propagation throughout the cementitious materials. Such data might be used to improve understanding of the mechanisms of crack development and distribution of cracks within the cementitious materials.

During fiscal year 2015, CNWRA staff performed a sequence of experiments to develop an understanding of the ultrasonic properties of tank grout and saltstone. The resulting property data were used to develop an AE monitoring technique capable of detecting and locating cracking events in the grout, which was demonstrated on a mesoscale specimen of tank grout during hydration. Ultrasonic experiments were performed using standard ultrasonic probes and driver instrumentation. Acoustic emission experiments were performed using a 16 channel Physical Acoustics Corporation DiSP Acoustic Emission Workstation, Model PCI–2 (i.e., an AE instrument), which was provided by Southwest Research Institute® Geosciences and Engineering Division. Two types of reducing tank grout and two types of non-radioactive saltstone were used to develop specimens for the experiments, where early experiments were conducted on proxy formulations of tank grout and saltstone until all materials necessary to develop DOE equivalent formulations became available.

Initial testing was performed on tall cylindrical specimens {70 mm [2.8 in] diameter and more than 200 mm [7.9 in] height} of each grout type to determine their ultrasonic properties in their hardened state. Ultrasonic through-transmission measurements were conducted using a variation of the method defined in Appendix X2 of ASTM E494. From these tests, tank grout was determined to have a nominal longitudinal wave speed of 4.14 mm/μs, a nominal shear wave speed of 2.9 mm/μs, and an approximate attenuation of 65–75 dB/m [20–23 dB/ft]. Saltstone was determined to have a nominal longitudinal wave speed of 2.39 mm/μs, a nominal shear wave speed of 1.13 mm/μs, and an approximate attenuation of 80–100 dB/m [24–30 dB/ft]. Both grout materials exhibited peak propagation amplitudes in the 100–150 kHz range and both materials permitted longitudinal wave signals to propagate with greater signal response than their shear wave counterparts.

The initial findings on the fully hardened specimens were used to define preliminary AE acquisition settings that could be tested on 1-to-2 L [1-to-2 qt] bench-top specimens of grout. Investigations were conducted by installing various configurations of AE sensors on the specimens and then performing ASTM standard E976 Hsu Nielsen source tests (pencil lead breaks) at known locations around their surfaces. The recorded pencil lead break signals were used to evaluate and refine AE sensor arrangement, acquisition settings, and data processing logic used to locate signal sources. Through initial refinement of the AE monitoring technique on the bench-top specimens, a sensor arrangement capable of detecting and locating pencil break events with an average error of less than 26 mm [1 in] (comparable to 1 wavelength) was selected.

An experiment was then performed to passively monitor the hydration process of a mesoscale, 108-L specimen of tank grout from initial placement through the first full month of hydration and hardening. The intent of the experiment was to evaluate the detection sensitivity and location capability of the AE monitoring technique against artificial crack sources throughout the grout hardening process and to collect ultrasonic property data throughout the grout hydration process. Given past experience with specimens of similar size, significant natural cracks were not expected to form, so artificial signals were periodically introduced via pencil break tests performed across the top surface of the specimen. Over the 32-day monitoring period, the AE system detected artificial signals with increasing consistency and accuracy. In the first few days of testing, signal detection and source location were prevented by high attenuation in the gel-like grout, which severely limited the measurement of key ultrasonic property data. By the end of the test, the system was demonstrating 100 percent detection of pencil lead breaks and location accuracy of less than 12 mm [0.5 in] across the top surface of the specimen. Further mesoscale experiments on tank grout and saltstone were delayed until the remaining ultrasonic property data could be collected on both materials using alternative experimental techniques.

In light of the severe attenuation observed in the mesoscale AE monitoring experiment, an additional experiment was devised to measure wave speed and attenuation throughout the grout hydration process. The method relies on performing periodic automated through-transmission tests on two specimens of grout with two known thicknesses and on a reference of water, using their relative signal responses and times-of-flight to calculate attenuation and phase velocity at each stage in hydration. The group velocity data could then be derived from the phase velocity data. Initial testing was performed on tank grout. Initial data indicate that there are two frequency bands conducive to AE monitoring—one in the 100–150 kHz range and a second near 50 kHz. Although detailed analysis of the velocities in these frequency bands was prevented by experimental complications, the phase velocities at higher frequencies were successfully captured, and attenuation response was consistent with previous test observations.

In future work, additional testing is required to complete characterization of the ultrasonic properties of tank grout and saltstone. Once the remaining required property data are established, CNWRA staff can optimize the AE monitoring technique. If AE-based crack detection and location is proven successful at the mesoscale, then the monitoring approach could be further refined for implementation on actual waste tanks for detecting cracks that may affect the capability of tank grout to provide a low-permeability reducing environment that limits release of key radionuclides.

ACKNOWLEDGMENTS

This report was prepared to document work performed by the Center for Nuclear Waste Regulatory Analyses (CNWRA®) for the U.S. Nuclear Regulatory Commission (NRC) under Contract No. NRC–HQ–12–C–02–0089. The activities reported here were performed on behalf of the NRC Office of Nuclear Material Safety and Safeguards, Division of Decommissioning, Uranium Recovery, and Waste Programs. The report is an independent product of CNWRA and does not necessarily reflect the views or regulatory position of NRC. The authors would like to thank G. Walter for his technical review and E. Pearcy for his programmatic review. The authors also thank L. Gutierrez for providing word processing support in preparation of this document.

QUALITY OF DATA, ANALYSES, AND CODE DEVELOPMENT

DATA: All CNWRA-generated data contained in this report meet quality assurance requirements described in the Geosciences and Engineering Division Quality Assurance Manual.

ANALYSES AND CODES: The computer software MATLAB®, AEwin, and LabVIEW were used in the analyses contained in this report. MATLAB, AEwin, and LabVIEW are commercial software controlled under Technical Operating Procedure (TOP)–018. Documentation for the Savannah River Site reducing tank grout and saltstone batches and for acoustic emission experiments can be found in Scientific Notebooks 1033 (Walter et al., 2015), 1226 (Puchot and Cobb, 2015), 1242E (Hooper, 2015), 1257 (Dinwiddie, 2010), and 1258E (Lenhard, 2015).

REFERENCES (for codes and notebooks)

Dinwiddie, C. Tank Grout and Saltstone Waste Release Acoustic Emission Testbed Experiments. Scientific Notebook No. 1257. San Antonio, Texas: Center for Nuclear Waste Regulatory Analyses. 2015.

Hooper, D. Saltstone and Tank Grout Batching and Specimen Preparation. Scientific Notebook No. 1242E. San Antonio, Texas: Center for Nuclear Waste Regulatory Analyses. 2015.

Lenhard, R. Saltstone Breakthrough Experiments to Investigate Potential Technetium Mobility. Scientific Notebook No. 1258E. San Antonio, Texas: Center for Nuclear Waste Regulatory Analyses. 2015.

Puchot, A and A. Cobb. Acoustic Emission Feasibility Study for Cementitious Materials. Scientific Notebook No. 1226. San Antonio, Texas: Center for Nuclear Waste Regulatory Analyses. 2015.

Walter, G., C. Dinwiddie, and D. Waiting. Small-Scale Grout and Grout Coring. Scientific Notebook No. 1033. San Antonio, Texas: Center for Nuclear Waste Regulatory Analyses. 2010.

UNIT CONVERSIONS

1 mm/μs = 3.94×10^{-2} in/μs
1 J = 9.48×10^{-4} Btu

1. BACKGROUND AND SCOPE OF REPORT

Large steel tanks are used to store liquid waste from processing nuclear materials as part of the defense programs of the U.S. Department of Energy (DOE). At the Savannah River Site (SRS), DOE has implemented a program to remove highly radioactive radionuclides from the tanks to the maximum extent practical and stabilize the residual waste using a cementitious chemically reducing grout. The purposes of the grout are to fill and structurally stabilize the tanks, and to provide a hydrologic and chemical barrier limiting the release of key radionuclides to the environment. Radionuclides that are removed from the tanks are encapsulated in another cementitious material known as saltstone, which is then permanently placed into underground vaults located at the Savannah River Site.

The U.S. Nuclear Regulatory Commission (NRC) previously sponsored studies at the Center for Nuclear Waste Regulatory Analyses (CNWRA®) to better understand the potential for cracks and other preferential pathways to form in tank grout monoliths particularly during the early years after grout is placed. Preferential pathways are of interest because they could allow rapid migration of water through the grout to the residual waste, limiting the chemical interaction of the water and the grout. Interaction between the water and grout is important because DOE's Performance Assessments assume that the grout chemically conditions the water to maintain the low solubility of key radionuclides and limit their release to the surrounding environment. As part of this study, CNWRA constructed an intermediate scale grout specimen inside of a 6.1 m [20 ft] diameter by 0.9 m [3 ft] high steel tank using reducing grouts similar to those intended for use at the Savannah River Site. The completed specimen was prepared in three grout placements over a 2-day period and reached a total height of approximately 0.8 m [2.6 ft]. During the construction and initial hardening of the specimen, several large cracks were observed to form on the exposed surfaces of the monolith. Many of the observed cracks formed during the first 24 hrs following grout placement. In subsequent assessment of the specimen, a total of 218 open cracks were characterized through various methods including laser topography measurement, water breakthrough inspection of the specimen wall (after removal of the steel tank), and core sampling. The cracks varied in dimension and in distribution across the surfaces of the specimen, implying multiple possible cracking mechanisms. A literature review of major cracking regimes was conducted and the characteristics of each crack regime were compared against the dimensions and placement of cracks found in the monolith. From this study, possible cracking mechanisms such as plastic shrinkage, plastic settlement, presetting, hydration shrinkage, thermal stress, and mechanical stresses were proposed as possible cracking mechanisms.

CNWRA is now providing technical assistance to the U.S. Nuclear Regulatory Commission (NRC) to test the feasibility of acoustic emission (AE) technology for passively monitoring crack formation within cementitious tank grout and saltstone, including during the early stages of hydration when the cementitious materials are in a gel form and challenging to monitor acoustically. Using AE sensors encapsulated by grout during grouting operations, it may be possible to passively monitor waste tank grout and saltstone monoliths for crack formation, record the timing and location of cracking, and map crack propagation. The timing and location information would be useful in diagnosing the mechanisms of crack formation and identifying the potential significance of the cracks for the performance of the grout.

Over the past 25 years, AE has seen increasing adoption by organizations such as the American Society of Nondestructive Testing and the American Society of Testing and Materials as a structural health monitoring technique for large mature concrete structures such as bridges, dams, and storage vessels. The existing monitoring practices assume that the structure has

reached working hardness prior to AE testing. Based on the early timing of crack formation in the intermediate-scale grout monolith, an effective AE monitoring technique for the subsequent studies must be able to detect crack formation early in the grout hydration process, including when the grout is in a gel form. Because acoustic attenuation in fresh grout is expected to be greater than in hardened grout and because the ultrasonic properties of grout are expected to change dramatically during hydration, monitoring grout throughout the hydration and setting process is more challenging than monitoring hardened grout.

For the purpose of this study, two cementitious materials, tank grout and saltstone, were investigated. The primary objectives for this feasibility study are to develop an AE monitoring technique to identify the timing and location of cracks that form within a grout monolith using commercially available AE equipment and to verify the technique on mesoscale test specimens. In addition, these tests have the following secondary objectives:

- Measure ultrasonic properties in fresh and fully hydrated grout
- Characterize propagating wave modes and changes in speed during initial stages of hydration and setting
- Characterize background signal sources produced by the hydration process
- Optimize the monitoring sensor configuration, instrumentation, and acquisition settings for the given materials and specimen geometry

If AE-based crack detection and location are proven successful on mesoscale grout specimens, then the monitoring approach could be further refined for implementation in the field.

This report provides a summary of the progress achieved by the CNWRA team during fiscal year 2015. Chapter 2 documents the materials used to develop tank grout and saltstone specimens and the acoustic emission sensors and equipment used to conduct AE testing. Chapter 3 documents the series of experiments that were undertaken, including their results. Chapter 4 presents a status summary of the work performed during fiscal year 2015 and conclusions reached. Chapter 5 presents CNWRA recommendations for completing this work during fiscal years 2016 and 2017.

2. MATERIALS AND EQUIPMENT

2.1 CEMENTITIOUS MATERIALS

At the U.S. Nuclear Regulatory Commission's (NRC) request, the U.S. Department of Energy (DOE) provided their vendor information for cementitious materials acquired by its contractor Argos (Jackson, South Carolina) for batching saltstone and Savannah River Site (SRS) reducing tank grout generally consistent with the LP#8–16 formula (Stefanko and Langton, 2013). At the Center for Nuclear Waste Regulatory Analyses (CNWRA®) request, the vendors (Holcim, Inc. and SEFA Group, Inc.) provided 55-gal drums of Portland cement I/II (ASTM C150), blast furnace slag cement (Grade 100, ASTM C989), and Class F Flyash (ASTM C618) for use in these experiments.

2.1.1 Savannah River Site Reducing Tank Grout

Two types of reducing tank grout were tested ultrasonically and acoustically during this reporting period. Preliminary tests were conducted on the deepest subsample of Core 12 that had been removed from the intermediate-scale grout monolith (Walter et al., 2010) on September 11, 2014, to obtain first-order material property information while staff awaited shipment of the materials required to prepare fresh specimens of DOE's selected grout formula (Stefanko and Langton, 2013). Hereafter, these grout types are referred to as Tank Grout Proxy and SRS Reducing Tank Grout (Table 2-1).

The Tank Grout Proxy formula used to develop the intermediate-scale grout monolith was based on a gravel-free formula reported for an alternative reducing grout in Langton et al. (2007) and Langton and Cook (2008). However, the reducing grout used in the intermediate-scale grout monolith was not identical to grout tested by Langton et al. (2007) because different vendors provided the Portland cement, sand, and fly ash. In addition, the quantity of water and Sika Viscocrete 2100 admixture used for the intermediate-scale grout monolith were adjusted to achieve specified slump flow with zero bleed and, thus, were not the same as used by Langton et al. (2007).

The gross composition of the Tank Grout Proxy differs from the final SRS Reducing Tank Grout in that the proxy material contains no coarse aggregate (gravel) that would enhance signal scattering and two of its three admixtures are completely different. For preparation of SRS reducing tank grout specimens during this reporting period, W.R. Grace and Company provided the following freshly prepared admixtures to CNWRA: (i) high-range water reducer ADVA Cast 575, (ii) high-range water reducer EXP–958, and (iii) hydration stabilizer RECOVER. The cementitious material, fine aggregate and water proportions are also different between the two tank grout formulas (Table 2-1).

For new bench-scale SRS reducing tank grout specimens, the cubic yard LP#8–16 (Stefanko and Langton, 2013) formula, modified in terms of its admixtures by Argos SRR–CWDA–2013–00026, 2014, was downscaled to be of an overall volume similar to that used previously to develop bench-scale saltstone specimens (Pabalan et al., 2013; Tables 2-2 and 2-3).

Table 2.1. Compositional and Material Vendor Information for 1-Cubic Yard Tank Grout Proxy and SRS Reducing Tank Grout Batches

Tank Grout Formula	Portland Cement Type I/II	Slag Grade 100	Fly Ash Class F	Quartz Sand	Gravel No. 8 3/8"	Water	ADVA Cast 575*	EXP–958*	Recover Hydration Stabilizer*	Sika Viscocrete 2100	Kelcocrete Diutan Gum
	lbs/yd^3					gal/yd^3	oz/yd^3				gm
Tank Grout Proxy†	303	303	790	1414	—	62.8‡	—	—	10	50§	217ǁ
SRS Reducing Tank Grout¶	125#	210#	363**	1790††	800‡‡	48.5§§	40¶	41.25¶	7¶	—	—

* W.R. Grace and Company, Columbia, MD
† Langton et al. (2007) and Langton and Cook (2008)
‡ Edwards Aquifer Well Water, San Antonio, TX
§ Sika Corporation U.S., Lyndhurst, NJ
ǁ CPKelco, Atlanta, GA
¶ Stefanko and Langton (2013) with admixture modifications per Argos batch tickets (SRR–CWDA–2013–00026, 2014). The preliminary AE tests described in Section 3.3 were conducted on a mesoscale grout specimen that was 1/7 of this batch size
# Holcim, Inc., Waltham, MA
** SEFA Group, Inc., Lexington, SC
†† South Carolina Minerals, Inc., North Augusta, SC
‡‡Aggregates USA, Grovetown, GA
§§Double-Deionized Water, San Antonio, TX

Table 2-2. Nominal Small-Scale Tank Grout Component Quantities per Batch*

Formula	Cementitious Materials				Water	w:c	Aggregate		Admixtures		
	Portland Cement Type I/II	Slag Grade 100	Fly Ash Class F	Total Cementitious Mass			Quartz Sand	Gravel No. 8	ADVA Cast 575	EXP–958	Recover Hydration Stabilizer
	grams								ml		
SRS Reducing Tank Grout	100	168	290.4	2954	323.2	0.58	1432	640	2	2	0.3

*Downscaled quantities are based upon Argos batch tickets provided for NRC review (SRR–CWDA–2013–00026, 2014)

Table 2-3. Nominal Small-Scale Saltstone Quantities per Batch

Saltstone Formula	Cementitious Materials				w:c	Water and Salt Mass (per Liter of Prepared Actual Salt Solution*)								
	Portland Cement Type I/II	Slag Grade 100	Fly Ash Class F	Total Cementitious Mass		Water	NaCl	NaOH*	$NaNO_3$*	$NaNO_2$*	Na_2CO_3*	Na_2SO_4*	$Al(NO_3)_3 \cdot 9H_2O$*	$Na_3PO_4 \cdot 12H_2O$*
	grams													
Saltstone Proxy†	180	812	812	3200	0.77	1396	314	—	—	—	—	—	—	—
Actual Saltstone*	100	450	450	1000	0.60	822.47	—	127.52	268.52	25.39	18.66	8.38	20.25	4.56

*Seaman et al. (2014); 882 g of saltstone solution is blended with 1000 g of premixed cementitious materials to produce a small batch of actual saltstone
†Pabalan et al. (2013); staff carried forward an apparent error from this reference whereby the total required salt mass of 307.75 g (Kaplan et al, 2008) was slightly overestimated, resulting in use of 314 g of NaCl in the saltstone proxy specimen

Fine aggregate (ASTM C33 sand) provided by South Carolina Minerals, Inc. was delivered in a bag on a pallet and was sensibly wet. For small grout specimens, this sand was oven dried prior to batch preparation. For the mesoscale preliminary acoustic emission test described in Section 3.3.2, sand was removed from the bag, spread on a tarp in the high-bay where batch mixing would occur and the experiment would be conducted, and allowed to dry with the aid of box fans directing air over the sand.

Other grout components were delivered in 55-gal drums including coarse aggregate (no. 8 stone or pea gravel) provided by Aggregates USA, as well as all cementitious materials. These materials were all sensibly dry and were not further dried.

To make each small batch of SRS reducing tank grout, the three cementitious materials were measured and premixed in a sealed, plastic Ziploc® bag until visually homogenized. The water and dry sand were measured and blended together in an 8-qt Globe® SP08 counter-top commercial kitchen mixer until homogenized, then the premixed cementitious materials were added to the wet sand and blending continued. The liquid admixtures were measured in pipettes or graduated cylinders and added to the bowl and blending continued. Then gravel was measured and added to the bowl for blending as a final step, to minimize resulting damage to the bowl. The fresh grout was poured into a cylindrical glass mold {70-mm inner diameter by 254-mm height [2.75 in by 10 in]} {or the bucket described in Section 3.2, which was also a 1-L [1-qt] batch} and allowed to harden, uncapped, for a minimum of 28 days. No attempt was made to keep an oxygen-free environment during preparation of the grout and it likely underwent some degree of oxidation during mixing and setting, particularly at the exposed surface of the column before the ultrasonic testing began.

Simple bases for the cylindrical glass molds were constructed using duct tape to secure plastic sheeting around one end of each mold; such bases were also used for the column specimens of saltstone discussed in Section 2.1.2. Prior to ultrasonic testing of the column specimens, the cylindrical glass molds were completely wrapped in duct or masking tape and hammered until the glass broke free from the specimen; this process was also used to free the column specimens of saltstone discussed in Section 2.1.2.

2.1.2 Saltstone

For the purposes of developing an acoustic emission (AE) monitoring technique, saltstone is an aggregate-free mixture of cementitious materials, water, and radionuclide-free salts. Two types of non-radioactive saltstone were tested ultrasonically and acoustically during this reporting period. To make progress on scoping tests for the experiments, a saltstone proxy specimen was developed during a period early in the fiscal year when the required high-purity laboratory grade salts were still being acquired from vendors. The saltstone proxy column specimen was prepared from dry cementitious materials (Type II Portland cement, Class F fly ash, and Grade 120 blast furnace slag cement) and a non-radioactive NaCl simulant of SRS tank waste solution using a formula based upon that of Kaplan et al. (2008) (Table 2-3). Once the lab grade salts had been obtained, a radionuclide-free saltstone column specimen was prepared using the actual saltstone formula of Seaman et al. (2014) (Table 2-3). For both types of saltstone simulant, the weight percentages of Portland cement, fly ash, and slag cement in the dry mix were 10, 45, and 45, respectively.

To make each batch of simulated saltstone, the three cementitious materials were measured and premixed in a sealed, plastic Ziploc® bag until visually homogenized. Each salt was

then measured and poured into a volumetric 1-L flask not quite filled to 1-L mark with double-deionized water. The salts were mixed in the flask until dissolved in the water.

Double-deionized water was added to bring the volume to precisely 1 L [1.06 qt], and then the required amount of salt solution and the premix (Table 2-3) were blended in a Globe® SP08 kitchen mixer. The resulting fresh saltstone was poured into (i) a cylindrical glass mold {70-mm inner diameter by 254-mm height [2.75 in by 10 in]}; (ii) two smaller cylindrical molds described in Section 3.1, one of which was subject to strict environmental controls; and (iii) a bucket mold containing a double batch, as described in Section 3.2, that was allowed to harden, uncapped, for a minimum of 28 days. No attempt was made to keep an oxygen-free environment during preparation and hardening of the saltstone and the specimens likely underwent some degree of oxidation, particularly at their exposed surfaces before the experiments began.

2.2 ACOUSTIC EMISSION EQUIPMENT

Southwest Research Institute® Geosciences and Engineering Division provided the use of its 16-channel Physical Acoustics Corporation DiSP Acoustic Emission Workstation, Model PCI–2 (AE instrument) for this investigation. The instrument was sent to the manufacturer for calibration and was returned on October 15, 2014, with a certificate of calibration. Upon return, the system was exercised to confirm functionality.

Due to the long lead times required to purchase AE probes, CNWRA selected a commercially available probe model for the study prior to the creation or testing of grout specimens. Without foreknowledge about the frequency response characteristics of the two grout materials, CNWRA opted to select an AE probe model that had a wide, relatively uniform operating frequency range. A literature review of other AE work conducted on gel-like grout indicated that peak signal detection occurred in the 100–200 kHz range (McLaskey, 2007; Chotard, 2003). Based on the available information, MISTRAS sensor model R15a was selected for this work. A representative frequency response for the probe model is shown in Figure 2-1.

The AE probes are connected to the AE instrument through individual preamplifiers with fixed selectable gain settings. The preamplifiers add 0, 20, or 40 dB of gain based on user selection, but otherwise are designed to pass signals detected by the AE sensor with minimal distortion.

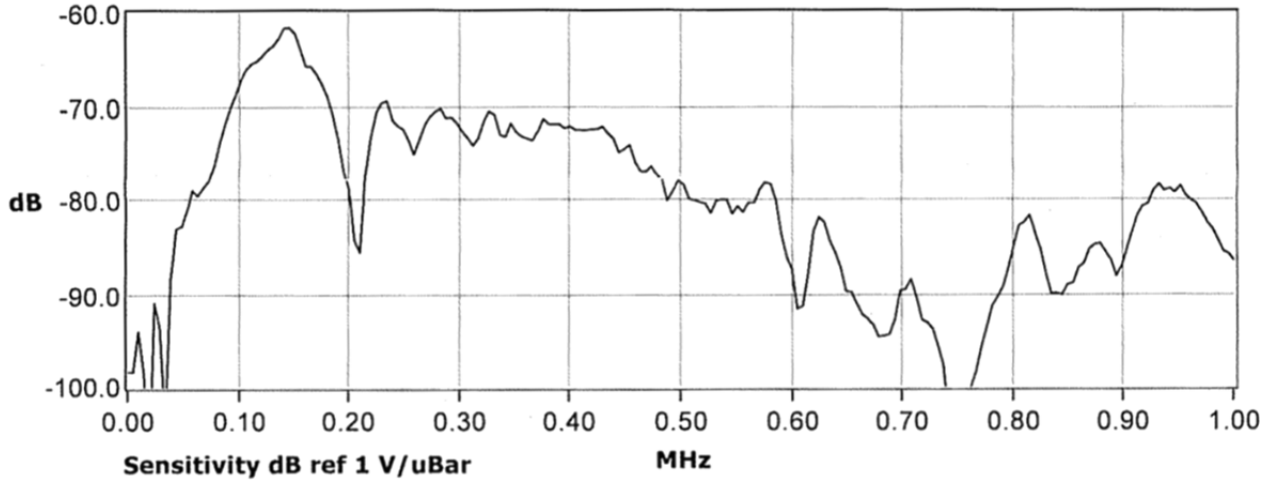

Figure 2-1. Frequency Response of MISTRAS R15a Acoustic Emission Sensor

3. EXPERIMENTAL METHODS AND RESULTS

A sequence of experiments was designed that would address the various secondary project objectives, concluding with a demonstration of acoustic emission (AE) monitoring on mesoscale specimens of tank grout and saltstone. The initial experiment would focus on measuring the basic ultrasonic properties of both materials in their hardened state. Once these property data were known, AE monitoring techniques would be investigated and refined on bench-scale specimens of hardened grout. After an AE monitoring technique had been established on hardened specimens, AE monitoring of a mesoscale specimen of grout would be attempted. During this experiment, the changes in ultrasonic velocity and attenuation would be characterized throughout the hydration and setting processes, and the AE monitoring technique would be further evaluated and refined. At the conclusion of the first mesoscale specimen test, an additional mesoscale test would be performed on each material, where the AE system improvements developed in the previous test would be applied.

In execution, the first mesoscale specimen test did not produce the ultrasonic property data as intended, so an additional ultrasonic property test was devised to acquire the property data and subsequent mesoscale tests have not yet been performed. Details regarding each of the experiments are described in the following sections.

3.1 ULTRASONIC TESTING OF HARDENED CYLINDRICAL SPECIMENS OF TANK GROUT AND SALTSTONE

The basic ultrasonic properties of each material were measured using a variation of the ultrasonic through-transmission testing method defined in Appendix X2 of ASTM E494. This test was primarily intended to accurately measure the longitudinal wave (L-wave) and shear wave (S-wave) speeds in a material, but was also useful for approximating the ultrasonic attenuation in the material for a given frequency range. In addition, measurements of ultrasonic waves generated in the frequency range that will be used for AE monitor were evaluated for spectral characteristics that could be used to define the AE monitoring acquisition settings. The test procedure involved propagating a series of ultrasonic waves through a long cylinder of hardened grout. The waves were generated and received by three matched pairs of piezoelectric ultrasonic transducers (Table 3-1).

Each matched probe pair was placed on either end of a cylindrical column of tank grout or saltstone, whose length was measured with a ruler. An ultrasonic pulser/receiver unit excited the transmitter probe, the receiver probe detected the propagating wave and the wave was amplified, and then recorded by an oscilloscope (Figure 3-1).

The captured waveform was digitally processed and reviewed to determine the ultrasonic time-of-flight and peak amplitude response. Once the measurement was performed with each pair of probes, a section of the specimen was removed from one end of the cylinder, and the measurements are repeated on the shortened cylinder. This procedure was repeated until the cylinder became too short to section further. A sectioned specimen is shown in Figure 3-2.

Table 3-1. Matched Ultrasonic Transducers for Through-Transmission Measurements

Brand	Model Number	Center Frequency	Wave Mode	Diameter (in)
Britek	BCC–1252	2.25 MHz	Longitudinal	1.00
Panametrics	V155	5.0 MHz	Shear	0.50
MISTRAS	R15a	150 kHz	Unconstrained	0.75

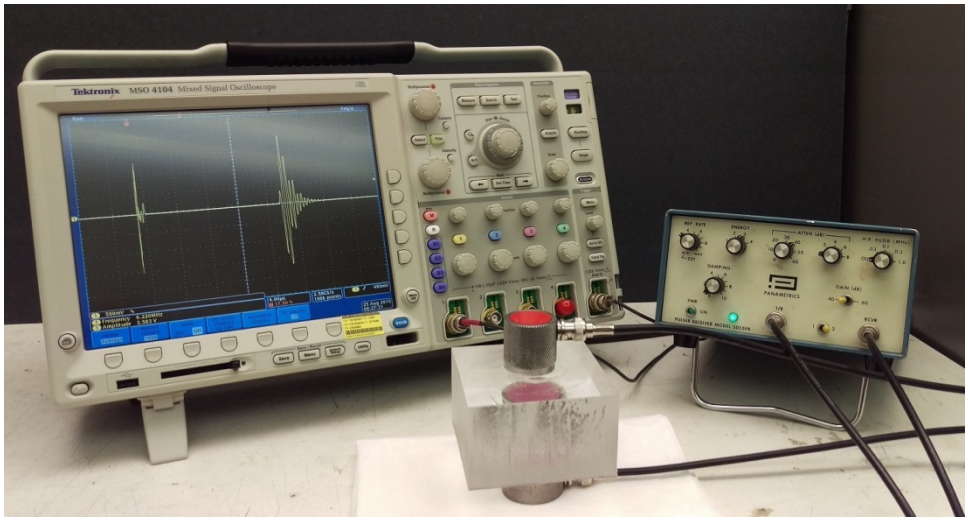

Figure 3-1. Equipment Setup for Ultrasonic Through-Transmission Measurement With Britek Transducers Positioned on Lucite Velocity Calibration Block

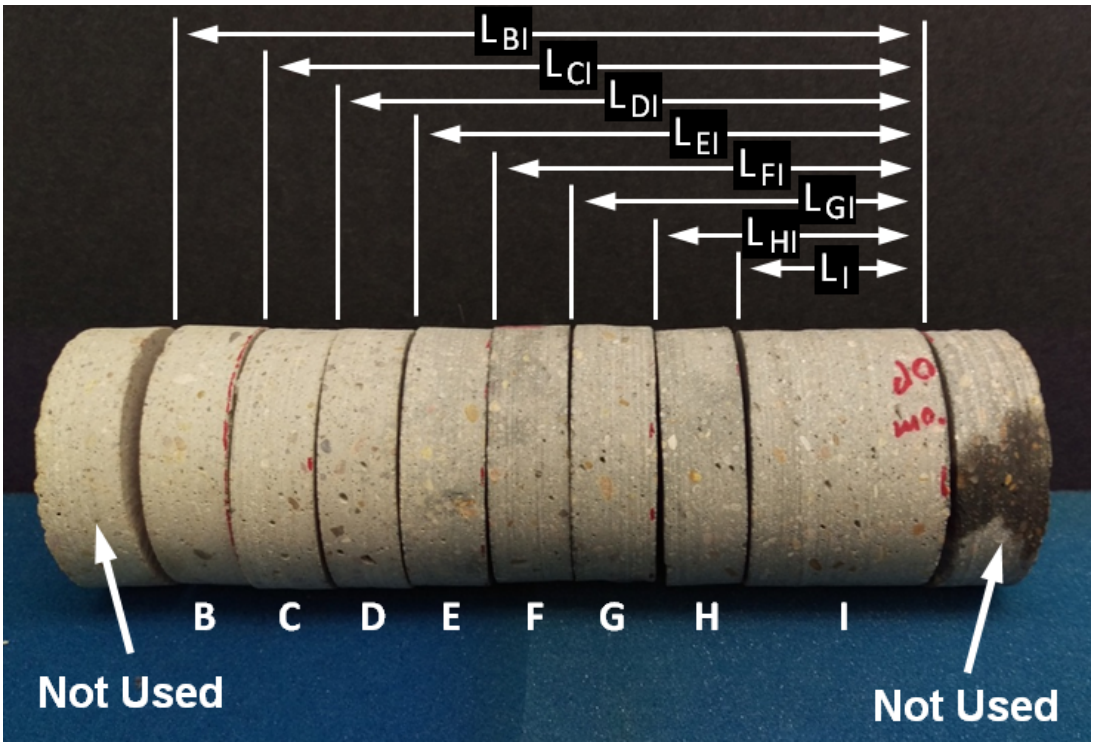

Figure 3-2. Sectioned Tank Grout Proxy Specimen After Ultrasonic Through-Transmission Testing; Upper End of Cylinder is to the Left

As sections were removed, the average L-wave and S-wave speeds through the remaining length of the specimen were calculated based on the remaining length of the specimen and the measured time-of-flight. Once the average wave speeds were calculated for each subsection (L-wave and S-wave speeds V_{bi} through V_{hi}), the local wave speeds in each subsection (V_B, V_C, ..., V_H, V_I) were calculated through the relation:

$$V_B = (L_{bi} - L_{ci})/(T_{bi} - T_{ci})$$

where V_B is the local speed for subsection B, L_{bi} and L_{ci} are the measured specimen lengths preceding and following subsection B, and T_{bi} and T_{ci} are the corresponding times-of-flight. Note that the relation is interchangeable for all subsections.

Approximations of ultrasonic attenuation through the grout are estimated by comparing the relative amplitude responses of the transmitted waves through specimen subsamples of different thicknesses. Because attenuation is frequency dependent, attenuation was calculated from measurements recorded from the AE probes to measure attenuation within the AE operating frequency range. Note that the estimates of attenuation made from these measurements are very approximate. The inconsistent transducer contact coupling with the nonuniform surfaces of the grout specimens tended to produce high variability in amplitude response. Because later testing was expected to produce more accurate attenuation values and because these initial attenuation estimates were only needed to estimate the monitoring coverage of each AE probe, the error was considered acceptable for this test. If more accurate attenuation information is required at some point, other testing methods should be considered.

Initial ultrasonic measurements were performed (i) on a deep subsample from Core 12 that was removed in 2014 from the intermediate-scale grout monolith, and (ii) on a saltstone proxy specimen. The intermediate-scale grout monolith was placed in three lifts on March 2–4, 2010, and has been continuously exposed to the elements since early April 2010, only being lightly covered by a plastic tarp when not under active examination (Walter et al., 2010). The saltstone proxy specimen set up and hardened under ambient laboratory conditions for 63 days prior to testing. Once cementitious materials procured from U.S. Department of Energy's (DOE) grout vendor's suppliers and saltstone salts were obtained, staff prepared authentic specimens of tank grout and radionuclide-free saltstone using DOE's formulas. These specimens were allowed to hydrate and set up under ambient laboratory conditions for at least 28 days prior to testing. Altogether, four ~1-Liter [1-qt] specimens of 70 mm [2.75 in] diameter and varying initial height were ultrasonically tested at this stage of the project: (i) tank grout proxy subsample from Core 12 {200 mm [7.9 in] height}; (ii) saltstone proxy with NaCl {205 mm [8.1 in] height}; (iii) Savannah River Site (SRS) reducing tank grout {215 mm [8.5 in] height}; and (iv) SRS radionuclide-free saltstone {215 mm [8.5 in] height}.

For the four ~1-L [1-qt] specimens tested, the waveforms transmitted in L-wave and S-wave modes exhibited roughly comparable attenuation rates, but signals transmitted in the S-wave mode were detected with substantially less amplitude than their L-wave counterparts. Over the largest propagation distances, the S-wave signals were typically too small to detect. In almost all cases, when the S-wave mode was detected, it presented amplitudes that were at least 30 dB smaller than the L-wave mode. For reference, Figure 3-3 compares the waveforms captured by the three pairs of probes after transmission through a 20 mm [0.8 in] section of tank grout. Based on the poor S-wave signal response, it is unlikely that S-waves will be detected during AE monitoring. The absence of the S-wave mode will simplify AE monitoring by eliminating the need to separate S-waves and L-waves for event detection.

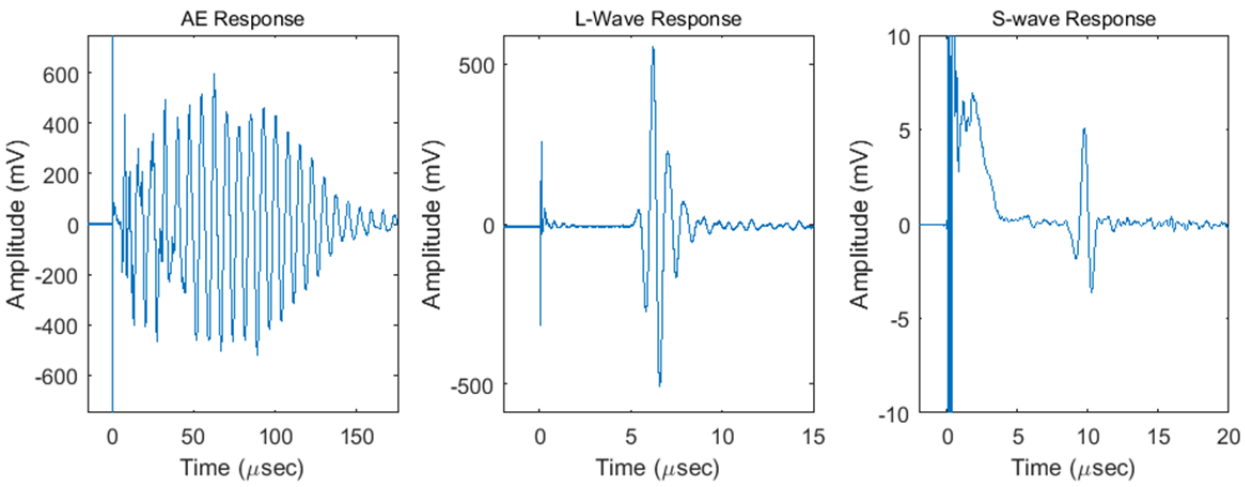

Figure 3-3. Comparison AE, L-Wave, and S-Wave Signals Captured After Transmission Through 20 mm [0.8 in] Section of SRS Reducing Tank Grout Specimen

Typical signals captured using AE sensors after transmission through SRS reducing tank grout and SRS radionuclide-free saltstone are shown in Figure 3-4. In both materials, the majority of the received signal had a frequency near 130 kHz. For tank grout, the main signal envelope (shown in cyan and green) tended to respond with a peak frequency of 130–140 kHz and bandwidth of 30–40 kHz. For saltstone, the main signal envelope (shown in cyan) tended to respond with a peak frequency of 120–150 kHz and a bandwidth of 25–35 kHz. The main signal envelope for saltstone was often less clearly separable from subsequent reverberations than for tank grout. The captured waveforms for both materials also exhibited low amplitude, broad bandwidth initiation signals that mark the first arrival of the wave. Because these initiation signals often exceed 10 μs in duration, accurate identification of these signals is critical to locating the position of acoustic events.

Calculated values for approximate signal attenuation and wave speed for each specimen are listed in Table 3-2. The values for signal attenuation and wave speed are fairly consistent for the two different specimens of tank grout. As expected for a specimen that is neither homogeneous nor isotropic, the L-wave speed varied notably through the thickness of the tank grout specimens. The observed attenuation rate also indicated that AE monitoring would be viable in tank grout over distances of a few meters.

Measurements from the saltstone proxy specimen yielded slower velocities than either of the tank grout specimens, but had similar rates of attenuation. Without the coarse and fine aggregate that is present in SRS reducing tank grout, the wave speed in saltstone was more uniform. A 3.8 percent variation was observed in the L-wave velocity of the saltstone proxy specimen, as opposed to a 5.7 percent variation in the tank grout proxy. Ultrasonic measurements from SRS radionuclide-free saltstone were not consistent with measurements from the saltstone proxy specimen. Compared to the saltstone proxy specimen, the SRS radionuclide-free saltstone specimen exhibited slower velocities and significantly greater attenuation. Further inspection of the SRS radionuclide-free saltstone specimen and other equivalent specimens produced at the same time revealed that the upper surfaces were deformable, friable and easily disintegrated into a sand-like substance. Discussions between U.S. Nuclear Regular Commission (NRC) and Center for Nuclear Waste Regulatory Analyses (CNWRA®) staff led to speculation that undesirable material properties were a consequence of allowing the specimen to harden under ambient conditions. It was hypothesized that the set-up

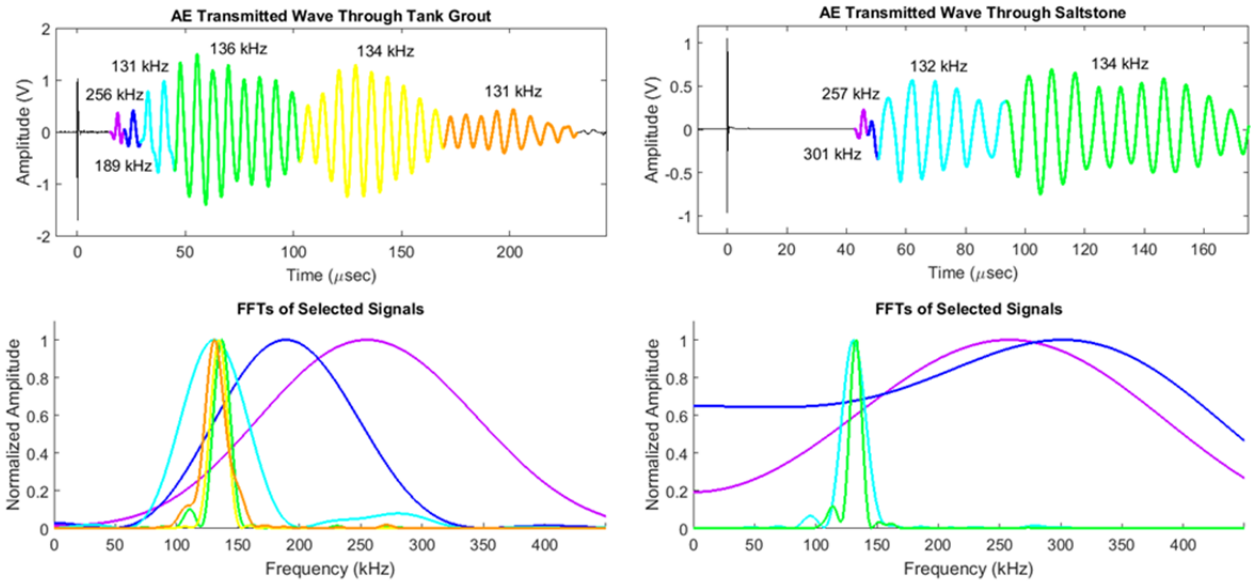

Figure 3-4. Typical Frequency Responses for AE Signal Transmitted Through SRS Reducing Tank Grout (Left) and SRS Radionuclide-Free Saltstone (Right)

Table 3-2. Attenuation and Wave Speed Data From Four Cylindrical Specimens

Material	Approximate Attenuation (dB/m) at 130 kHz	L-wave Speed (mm/μs)	S-wave Speed (mm/μs)
Tank Grout Proxy (Core 12 Subsample)	60–80	4.20 ± 0.24	2.50 ± 0.07
SRS Reducing Tank Grout	65–75	4.14 ± 0.26	~ 2.9
Saltstone Proxy (NaCl)	70–90	3.16 ± 0.12	1.65 ± 0.12
SRS Radionuclide-free Saltstone	>200	2.29 ± 0.05	0.95 ± 0.03

time for saltstone may exceed that of tank grout, which may cause variations in ultrasonic properties of the material to develop several weeks after initial hardening.

Another cylindrical specimen {3.8-cm diameter by 10.2-cm height [1.5 in diameter by 4 in length]} of SRS radionuclide-free saltstone prepared in late-April 2015 had been allowed to hydrate and harden inside an environmentally controlled chamber for approximately 2 months. An ESPEC Temperature and Humidity Bench Top Chamber BTL–433 environmental chamber with an initial temperature of 25 °C [77 °F] was used. The chamber was pre-programmed with a protocol provided by NRC to increase the temperature 5 °C [9 °F] per day until a maximum of 65 °C [149 °F] was obtained. After attaining the peak temperature, it was held constant for 14 days, after which the temperature was reduced 5 °C [9 °F] per day until reattaining the initial temperature. The humidity was held constant at 100 percent throughout the duration of this 30-day hardening process. After the active temperature control protocol had been completed, this specimen remained in the chamber for approximately another full month. Excess material from the same saltstone batch was poured into a second mold and allowed to hydrate and harden under ambient laboratory conditions. CNWRA staff decided to commit the environmentally controlled specimen to destructive ultrasonic testing for the dual purposes of determining the severity of ultrasonic attenuation in saltstone and determining if the ultrasonic properties of saltstone are stable during later stages of hydration. To evaluate attenuation,

ultrasonic through-transmission data were collected from the environmentally controlled saltstone specimen and compared against data collected from the other available saltstone specimens. To evaluate the stability of the ultrasonic properties, this sectioned saltstone specimen was stored and retested five weeks later.

The environmentally controlled SRS radionuclide-free saltstone specimen was sliced into four sections perpendicular to its axis. The uppermost section had been exposed to free-standing salt solution during setting and did not have the solid consistency of the other sections, so it was abandoned for testing. The remaining three sections were tested using a simplified version of the ultrasonic through-transmission technique. Because all measurements would be compared at two points in time and the specimen could not be rejoined after sectioning into subsamples, through-transmission measurements were simply recorded on each individual sliced section. Between the initial measurements and the second set of measurements, its sections were placed in a plastic canister and partially submerged in deionized water to a depth of roughly 6 mm [0.2 in]. The canister was brought to near vacuum and repeatedly purged with 99 percent pure nitrogen. After a week of observation, some of uppermost section appeared to partially dissolve into the water. After 13 days, the storage plan was revised to prevent possible damage to the subsamples. A bed of glass beads was added to the canister with a depth of 70 mm [2.75 in]. The canister was then refilled with deionized water to a depth of 40 mm [1.6 in], and the subsamples were positioned on the glass bed. Again, the canister was purged with nitrogen and sealed.

As indicated by the velocity results shown in Table 3-3, the wave speeds in the environmentally controlled specimen remained effectively constant between measurements. For reference, the ambient specimen created using the excess material exhibited an L-wave velocity of 2.27 mm/μs and an S-wave velocity of 0.99 mm/μs, which is consistent with the previously measured SRS radionuclide-free saltstone specimen that set up under ambient laboratory conditions.

Signals recorded in the S-wave mode, which are anticipated to be poorly supported in saltstone based on prior testing, exhibited comparable amplitudes in both the environmentally controlled specimen and the uncontrolled excess material specimen from the same saltstone batch. Signals recorded in the L-wave mode exhibited significant differences. The amplitude response data collected on the environmentally controlled specimen indicated that ultrasonic attenuation is in the range of 80–100 dB/m [24–30 dB/ft]. Comparisons of the signal response in the environmentally controlled specimen to other previously measured saltstone specimens, confirmed this attenuation estimate. Based on this attenuation, which is roughly half the attenuation observed in the saltstone specimen that had set up under ambient conditions, it is reasonable to assume that ultrasonic and other material properties of saltstone are highly dependent on environmental conditions during hydration. For reference, a comparison of the wave speeds measured in the various representative saltstone specimens is provided in Table 3-4.

Table 3-3. Wave Speeds Measured in Environmentally Controlled Specimen of SRS Saltstone			
Measurement Date	**Specimen Age**	**L-wave Speed (mm/μs)**	**S-wave Speed (mm/μs)**
July 14, 2015	75 Days	2.38	1.12
August 21, 2015	113 Days	2.39	1.13

Table 3-4. Attenuation and Wave Speed Data From SRS Radionuclide-Free Saltstone Specimens and NaCl Proxy Specimen Hardened Under Various Conditions			
Material	**Approximate Attenuation (dB/m) at 130 kHz**	**L-wave Speed (mm/μs)**	**S-wave Speed (mm/μs)**
Saltstone Proxy (NaCl)	70–90	3.16 ± 0.12	1.65 ± 0.12
Cylindrical Saltstone Specimen Hardened at Ambient Temperature	>200	2.29 ± 0.05	0.95 ± 0.03
Cylindrical Saltstone Specimen Hardened Under Environmentally Controlled Conditions	80–100	2.39	1.13
Excess Saltstone Hardened Under Ambient Conditions (same batch as above)	N/A	2.27	0.99

3.2 ACOUSTIC EMISSION EVALUATION OF HARDENED, BENCH-SCALE MONOLITHS

Initial AE performance investigations were conducted on small, 1-to-2-L [1-to-2-qt] bench-top specimens of SRS reducing tank grout and proxy saltstone to establish preliminary guidelines for AE acquisition settings, sensor arrangement, and data processing logic that could be applied to larger monoliths during later experiments. Investigations were conducted by installing various configurations of AE sensors on the specimens and then performing ASTM standard E976 Hsu-Nielsen source tests (pencil lead breaks) around their surfaces (ASTM E976–10). A pencil lead break on a surface produces a strain impulse response by momentarily loading the surface and then suddenly relaxing. The strain impulse response produces a broad spectrum acoustic wave that can be measured by the AE system to provide performance metrics regarding detection sensitivity and location accuracy, as well as spectral characteristics of the propagating signal itself. Pencil break tests provide a reasonably repeatable method of testing the signal response in a specimen where the timing and location of the signal source is known. The tests are limited in that they can only be performed at the grout surface and there is limited control in the wave motion produced by the break. The pencil break tests also require a hardened surface.

Automated Sensor Tests (AST) were also performed on each specimen to measure the wave speed. In an AST, each AE channel is actively pulsed in sequence. As each channel is pulsed, the other sensors record the transmitted wave. At the completion of an AST, an ultrasonic wave has been transmitted in both directions between each possible sensor pair on the specimen. Although the L-wave and S-wave speeds were already determined from the ultrasonic

through-transmission tests, reduced velocities were anticipated in the bench-top specimens due to their small size. The L-wave signals detected by the AE sensors have wavelengths ranging from roughly 10 to 100 mm [0.4 to 4 in] in these specimens. Because a large fraction of the signals are received with wavelengths that are comparable to the specimen dimensions, the signals interact with the specimen boundary and velocity dispersion occurs. To eliminate contributions from signals with the longest wavelengths, the highpass filter cutoff was increased from 1 to 20 kHz for these tests. For larger specimens, this highpass filter cutoff may be reduced.

The two bench-top specimens were cast in half-gallon buckets to achieve an approximately cylindrical form factor similar to the larger mesoscale specimens that would be tested in later experiments (Figure 3-5). Both bench-top specimens were allowed to set up under ambient laboratory conditions. As the saltstone proxy specimen set up, salt precipitated out of the saltstone and formed a layer of crystals covering the upper surface. After one month, the specimen was removed from the bucket, and the top surface was sanded smooth. A network of hairline cracks was observed around the side and bottom surface of the specimen. The SRS reducing tank grout specimen was removed from the bucket after one month of hydration and required no additional surface preparation. No visible cracks or loose aggregate was observed to break the surface of the specimen, but a number of small vesicles were observed around its circumference. The dimensions and wave speeds of both specimens are provided in Table 3-5, where wave speed was measured using a simplified variation of the ultrasonic through-transmission technique discussed in Section 3.1.

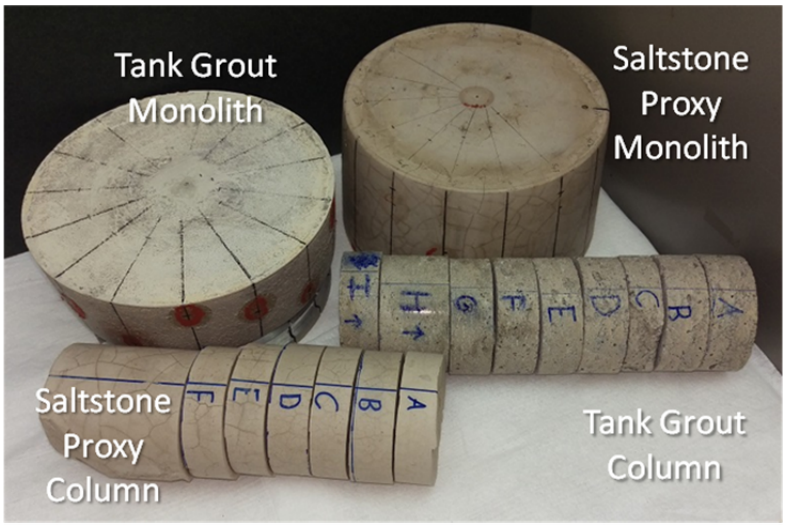

Figure 3-5. Photograph of Bench-Top Monoliths and Sectioned Cylinders of Tank Grout and Proxy Saltstone

Table 3-5. Dimensions and Measured Wave Speeds of Bench-Top Grout Specimens

Specimen	Upper Diameter (mm)	Lower Diameter (mm)	Height (mm)	Estimated Volume (L)	L-wave Speed (mm/μs)	S-wave Speed (mm/μs)
Tank Grout Proxy	170	177	54	1.28	4.30	2.84
Saltstone Proxy	166	184	99	2.38	3.16 ± 0.02	N/A

The saltstone proxy specimen was preferred for bench-top testing due to its earlier availability and larger size. Initially, one AE sensor was installed at the top center of the specimen and four additional sensors were installed at cardinal points around the circumference at about the mid-height. Pencil lead breaks were performed across the top surface. Typically, the pencil breaks exhibited centroid frequencies in the range of 80–120 kHz and absolute energies on the order of 100 µJ.

Various AE sensor configurations were applied to the saltstone proxy specimen. Preliminary evaluations of the capability of a configuration to detect and locate crack events were made by performing pencil breaks on the top, bottom, and side of the specimen and by evaluating the detection rate and location accuracy of the recorded events. The studied sensor configurations focused heavily on placement of the sensors on the wall of the specimen. Note that without refined AE acquisition settings, a rigorous evaluation of each sensor configuration could not be made at this point in testing. Illustrations of some alternative sensor layouts are shown in Figure 3-6, where sensor placement is illustrated as an overhead view and as an "unwrapped" side view of the specimen.

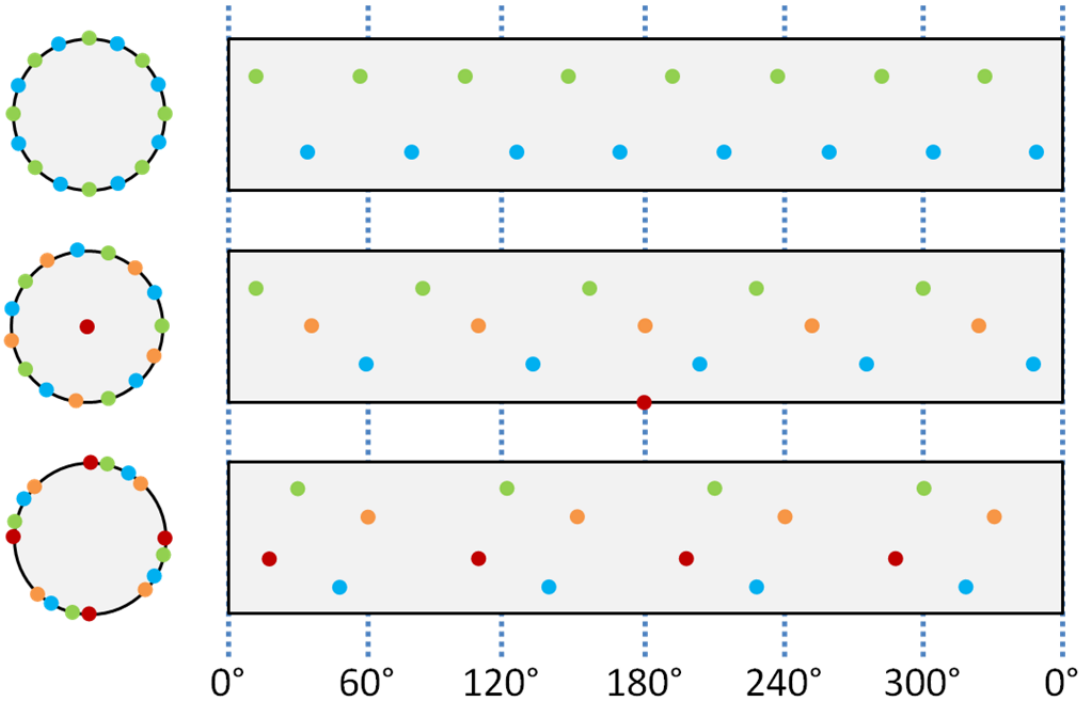

Figure 3-6. Alternative AE Sensor Arrangements Around Circumference of Cylindrical Grout Specimens

The upper arrangement illustrated in Figure 3-6 shows the sensor configuration that was originally recommended for the specimens. It consists of two bands of eight AE sensors that are staggered in clocking position. While this arrangement offers good detection coverage, the arrangement lacks redundancy in overlapping coverage needed for accurate event location. The alternative shown in the lower arrangement solves this by positioning sensors in tighter clusters about the circumference of the specimen. This method improves the location accuracy of many, but not all, detected events, but exhibits inferior detection coverage. The middle arrangement (Figure 3-6) improves upon the location accuracy of the upper arrangement while still maintaining comparable detection coverage over the specimen. At the time of the test, the middle arrangement had also been tested in a preliminary fashion on the mesoscale test stand that was being developed for later experiments, so it was somewhat more refined in implementation than the other configurations. This arrangement proved to provide both a high rate of event detection and appeared to be the configuration that was most likely to locate events accurately once the AE system had been appropriately tuned.

Installation of the AE system on the saltstone specimen was completed, as shown in Figure 3-7. An AST was performed, where each AE sensor was actively pulsed in sequence and every other sensor recorded the transmitted wave. Using the resulting data set, estimates of wave velocity through the specimen were made. The AST returned an average velocity of 2.75 mm/μs.

Pencil break tests were performed at known locations across the top surface of the specimen while the AE system recorded events. Afterward, the location data were reprocessed using several different assumed wave velocities between 2.5 and 3.5 mm/μs to determine which velocity produced the least location error. Through this “trial and error” method, the AE location algorithm produced greatest location accuracy with an assumed velocity of 2.75 mm/μs. Using this assumed velocity, additional location accuracy tests were performed around the side of the specimen. Throughout testing, the largest remaining component of location error appeared to occur in depth, particularly when pencil breaks were performed across the top

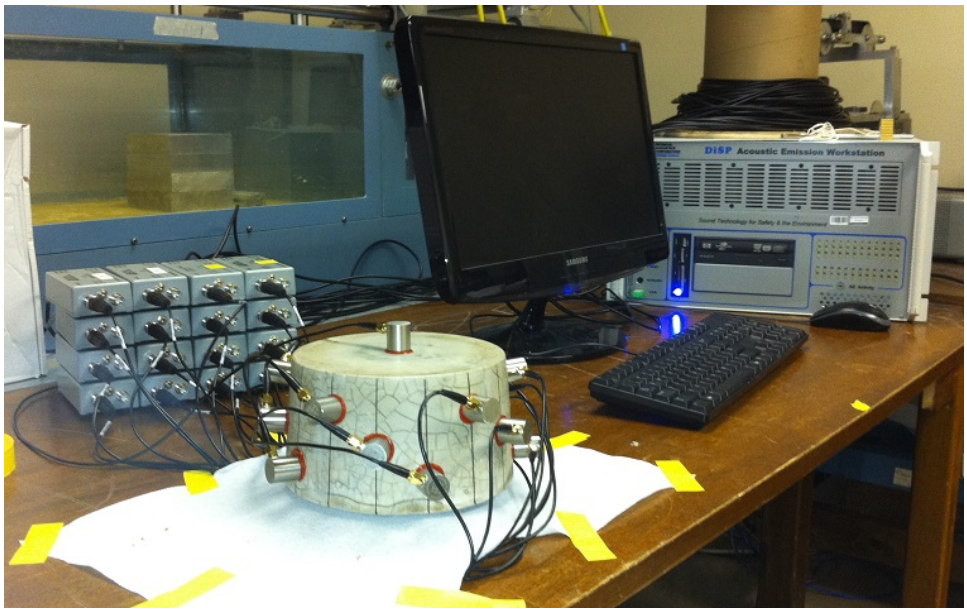

Figure 3-7. AE Experimental Setup on Bench-Top Saltstone Proxy Specimen

surface of the specimen outside of the enclosed coverage of the sensor grid. This error appears to be produced by a limitation in the implemented location algorithm.

To help reduce this error, the upper and lower band of AE sensors were repositioned closer to the top and bottom surfaces of the specimen to increase the volume of the specimen enclosed by the sensor network. After repositioning the sensors, pencil break tests were repeated, and the system was able to locate events on the top surface of the specimen with an average position error of less than 20 mm [0.8 in]. This error corresponds to a distance of one wavelength at the typical wave propagation speed and signal frequencies in the specimen.

The selected AE sensor configuration was also installed on the bench-top SRS reducing tank grout specimen and pencil breaks were performed to determine characteristic signal responses in this material. The pencil breaks exhibited centroid frequencies in the range of 100–140 kHz, but also exhibited a secondary band of peak frequencies in the range of 40 kHz. The presence of this secondary frequency band indicates that if AE monitoring in the 100–140 kHz is not successful, AE probes could be selected that are better tuned to receive signals in the 40 kHz frequency range. The absolute energies of detected pencil breaks often exceeded 1000 μJ, or ten times the energy levels detected in the saltstone proxy material.

An AST was performed on the bench-top SRS reducing tank grout specimen, and an average L-wave velocity of 3.90 mm/μs was calculated. Using this assumed velocity, location accuracy tests were performed by monitoring the specimen while making pencil lead breaks around the top surface and side of the specimen at known locations. The average position error for the detected pencil lead breaks was less than 26 mm [1 in], or approximately one wavelength at the typical wave speed and signal frequencies in the specimen.

3.3 AE MONITORING OF HYDRATING MESOSCALE SRS REDUCING TANK GROUT MONOLITH

Concurrent with other experiments, CNWRA staff began preparations for the first of three mesoscale experiments during which 108 L [28.5 gal] specimens would be AE monitored from initial placement through the first full month of hydration and hardening. In prior experiments, various ultrasonic property data had been collected on fully hardened specimens of tank grout and saltstone. The intent of the mesoscale tests was to measure the ultrasonic velocity and attenuation throughout the process and to demonstrate AE detection and location of signals within the cementitious material at various stages in its evolution.

NRC and CNWRA staff agreed that a specimen of SRS reducing tank grout would be subject to acoustic emission testing first to rapidly advance understanding using the least expensive materials (i.e., no high-purity salt), and that a saltstone specimen would be tested subsequently based upon those initial lessons learned. In total, CNWRA anticipated conducting these experiments on two specimens of SRS reducing tank grout and then conducting a third such test on SRS radionuclide-free saltstone. Each test would provide data on the variation of ultrasonic velocity and attenuation throughout the hydration and setting process.
The monitoring data from each test would also be used to measure and characterize any acoustic signals produced by the process that are unrelated to cracking events (Lura, 2009).
It is important to identify extraneous signals to prevent potential false identification of crack signals in larger field-scale test specimens.

The first mesoscale specimen test also included objectives related to evaluation of the AE system implementation. Throughout the first test, the monitoring data were reviewed and AE

acquisition settings were evaluated and refined to improve monitoring performance and to identify potential shortcomings in the AE monitoring technique. After completion of the test, the AE system implementation was evaluated for detection sensitivity and location accuracy. The evaluation results may be used at a later point to modify the AE implementation on subsequent tests.

3.3.1 AE Mesoscale Test Fixture

An AE test fixture for monitoring grout was constructed by installing a series of sensor mounts into a 360 L [95 gal] high density polyethylene overpack drum (Figure 3-8). The probe mount configuration consisted of three bands of five probe mounts spaced evenly around the circumference of the drum. The bands are positioned at heights of 51, 152, and 254 mm [2, 6, and 10 in] relative to the base of the drum. Each band of probe mounts is circumferentially staggered by 24° from the preceding band. Viewed from overhead, there are 15 probe positions clocked at 24° intervals about the circumference of the drum, designated CH01 through CH15. A final probe, designated CH16, is centrally located at the base of the drum.

Each AE probe is held in place by a spring-loaded probe mount (Figure 3-9), similar to the setup described by Abeele et al. (2009). As the specimen expands and contracts throughout the hydration process, the spring ensures that the probe remains in contact with the specimen. The probe is coupled to the grout through a thin plastic film fitted between the fixture and the specimen that is attached to the probe face by a thin layer of room temperature vulcanization silicone.

Figure 3-8. Acoustic Emission Test Fixture (Left) and SRS Reducing Tank Grout in Test Fixture Bucket (Right)

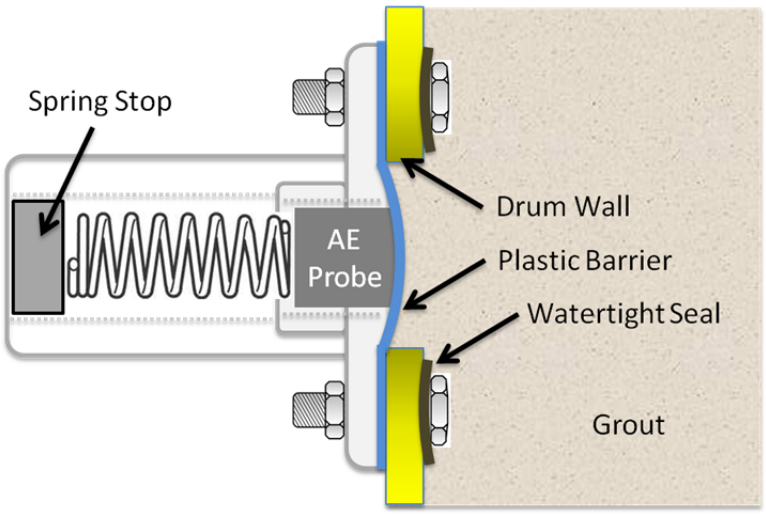

Figure 3-9. Spring-Loaded AE Sensor Mount

A 108 L [28.5 gal] batch of material would fill the drum to an approximate depth of 315 mm [12.4 in] and would measure 660 mm [26 in] in diameter. The specimen dimensions were selected to prevent velocity dispersion from occurring due to signal interactions with the boundaries of the grout.

The entire fixture is mounted on a reinforced shipping pallet and raised on cinder blocks. The raised pallet provides access to the lower AE sensor and helps to insulate the bucket from low frequency noise that may propagate through the concrete floor in the high bay where it is located.

3.3.2 AE Monitoring Log for Preliminary Tank Grout Specimen

Once sufficient data had been collected about the ultrasonic properties of the tank grout and saltstone materials and a basic AE monitoring technique had been developed and tested on bench-scale, hardened specimens, CNWRA staff mixed a ~108 L [28.5 gal] batch of SRS reducing tank grout and transferred it to the AE test fixture. The fresh grout filled the drum to a depth of 295 mm [11.6 in]. Immediately after pouring, an AST was performed to verify sensor operation and establish the initial ultrasonic properties of the gel-like specimen. In its fresh state, the grout was not able to support the signal transmitted by AST, so the sensors were triggered instead by a forceful impact to the top surface of the grout. After verifying sensor operation, the AE system was placed in a continuous monitoring state. The monitoring period was anticipated to last one month. During this timeframe, the 16 AE channels captured all signals that exceeded a fixed detection threshold, which was initially set to 55 dB_{AE}. In addition to AE monitoring, an automatic AST was periodically performed. In the first 10 days, ASTs occurred in 1-hr intervals. Afterward, the interval was increased to 6 hrs. Because natural cracks were not expected to form in this specimen, the AE monitoring system was occasionally paused to perform pencil lead break tests on the top surface. The artificial crack signals produced by these tests were saved separately to evaluate location accuracy and event detection sensitivity at different stages during the grout hydration process.

During the first 18 hrs after the grout pour, the AE system detected only 32 minor signal hits, (Figure 3-10; Table 3-6). Monitoring was briefly paused to conduct pencil lead break tests to check sound propagation. Testing confirmed that induced sound readily propagated to multiple sensors that are in contact with the material. Therefore, the paucity of signals indicated that the early stages of setting and hydration were not very noisy. This implied that monitoring grout for cracking during this early stage should be effective because there should be few extraneous signals that could be confused with cracking.

Nearly 2 days after the grout pour, 84 unique acoustic signals were detected over a timespan of approximately 14 hrs (Figure 3-10; Table 3-6). The energy levels of these signals were low (i.e., on the order of 10 nJ) and the event locations therefore remained indeterminate because they were generally only detected by a single sensor, rendering triangulation impossible. It can be inferred that these events were probably located close to the single sensor that detected them. Acoustic signals of this type shared several common identifying features and should be distinguishable from more typical cracking signals.

Over the next several days, two additional pencil lead break tests were performed to check sensor operation and detection sensitivity, but the grout specimen showed no further signs of notable AE events. After 10 days of testing, sufficient data had been collected on the test specimen to permit modification of the acquisition system settings to improve the instrument sensitivity by 15 dB. Monitoring for the remainder of this test continued with the revised acquisition settings. On April 24, an operating system failure caused the AEwin monitoring software program to close (Figure 3-10; Table 3-6). Once this problem had been identified, the monitoring program was reset and resumed monitoring from May 6 through May 12 (Figure 3-10; Table 3-6).

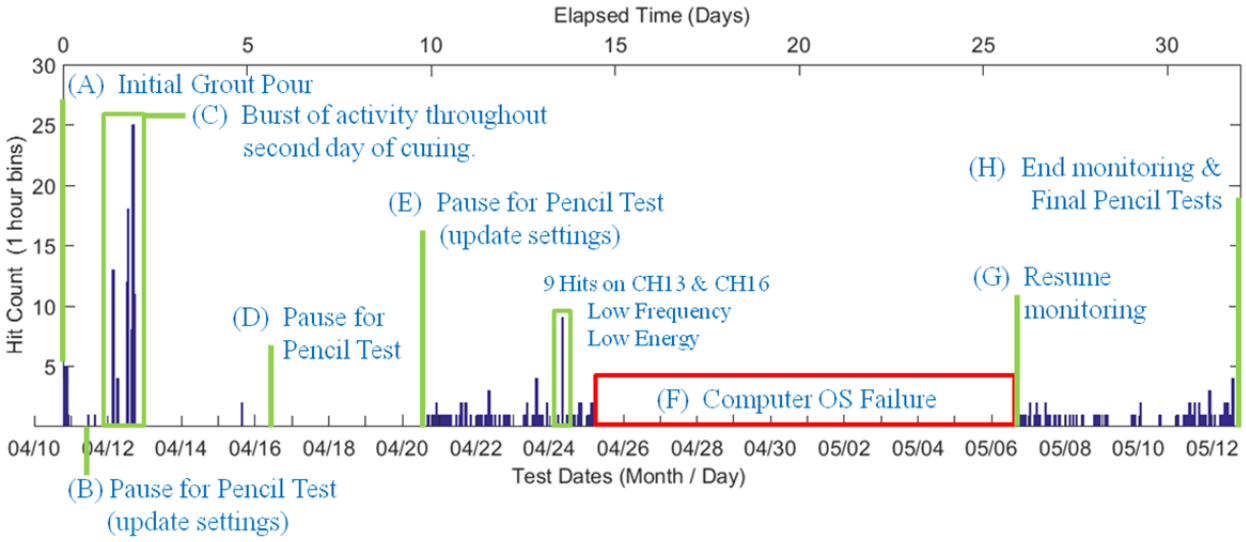

Figure 3-10. AE Hit Activity Log Shown as a Timeline Over 32-Day Monitoring Period

Table 3-6. Key Events During 32-Day AE Monitoring Period		
	Event and Time	**Description**
A	Initial Grout Pour (04-10-15 @ 19:04)	Tank Grout poured by 5-gal bucket in 12 batches totaling roughly 101 L [107 qt]. Final grout depth roughly 295 mm [11.6 in]. Grout allowed to settle, then manual ASTs performed. Signals were not observed to propagate though the material, so initial attenuation was very high. Sensor operation was confirmed via impacts to the top surface of the grout. After settling, AE monitoring began.
B	First Pencil Break Test (04-11-15)	Grout already observed to have a solid consistency, although a water film was observed above the top surface. Observations from pencil breaks were used to update settings to improve AE waveform capture.
C	Burst Sequence Hits (04-12-15 @ 3:52)	A relatively high level of AE activity is detected between 33 and 47 hrs into AE monitoring. 84 hits are detected during this period, but all hits are low energy. The hit presentation also exhibits an unusual burst sequence, where repetitive signals with fairly consistent acoustic characteristics are detected several times in a few seconds by a single channel at a time.
D	Second Pencil Break Test (04-16-15)	No other activity noted.
E	Third Pencil Break Test (04-20-15)	Revisions made to acquisition settings based on data collected to date resulted in 15-dB improvement in signal sensitivity. Acquisition settings updated. Note that after this update, the AE hit detection rate increased, but almost all of the detected hits are low energy signals below the previous detection threshold.
F	Computer OS Failure (04-24-15 @ 12:54)	Automatic updates inadvertently restored; computer attempted to update and failed, causing reboot. AE monitoring program did not reinitialize at reboot.
G	Resume Monitoring (05-06-15 @ 14:47)	Failure detected and investigated. Cause of failure corrected and monitoring program resumed.
H	Conclude Monitoring & Final Pencil Break Test (05-12-15 @ 14:47)	Elapsed test duration met and no acoustically significant hits noted since previous review of system (G), so test concluded. Pencil breaks performed across the top surface are detected evenly by the majority of sensor channels. Acoustic velocity is noted to be near the hardened bulk wave velocity measured in preliminary tests.

3.3.3 Monitoring Outcome for Preliminary Tank Grout Specimen

Preliminary review of the monitoring results indicated that the only significant AE activity occurred over a 14-hr span on the second day. The low energy AE hits recorded during this timeframe occurred in a rapid sequence of bursts that were detectable only on individual channels at any given time. Energy levels of these hits were typically less than 0.2 μJ, and the signals had distinct spectral characteristics, including:

- Short waveform duration – less than 100 μs
- Very low peak frequency – most commonly 8 kHz, but some at 17 kHz and 42 kHz
- Low centroid frequencies – typically ranging from 65 to 85 kHz.
- Highly repetitive – similar waveforms detected several times in a few seconds.

The burst sequence phenomenon was observed by 8 of 16 AE sensors at different times. The detection sequence began in the top sensor row and ended in the bottom sensor row. An illustration of the order of the burst sequence is shown in Figure 3-11. Given their low energy levels, these hits are suspected to have been generated by minor source events that were located near the detecting sensors. It is possible that a larger number of these source

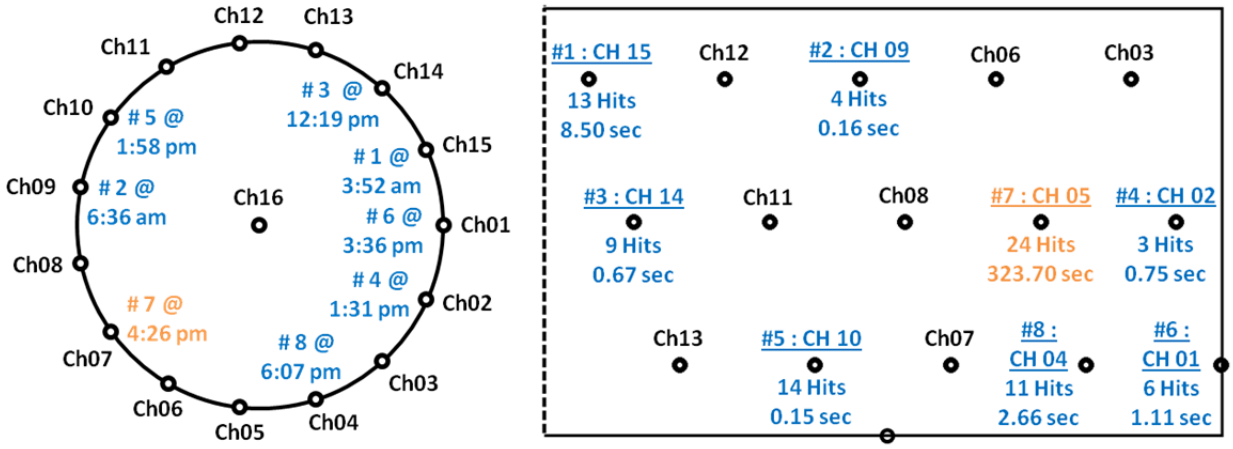

Figure 3-11. Illustration of Burst Sequence Phenomena Recorded on Second Day of Monitoring, Shown in Overhead and Unwrapped Views

events occurred within the grout but remained undetected due to low energy levels. Given the attenuation present within the grout at the time of these hits, it is also possible that these hits were generated by cracking events within the grout, but this is doubtful because the spectral characteristics of these signals are atypical of crack signals and because pencil breaks at the top surface had already shown to be successful prior to the detection of these hits. Although the source of these signals may merit further study at some point, for the purpose of this work, they can be ruled out as crack signals and will therefore most likely be removed from the AE monitoring data set in future tests.

The grout specimen appeared to become nearly acoustically inactive after the second day of monitoring. Between April 12 and April 20, two pencil break tests were performed, but AE hits were sourced from the grout specimen itself. After the April 20, 2015, sufficient data had been collected from pencil break tests to improve the AE acquisition settings. Through improvements to the waveform timing capture logic and adjustments to the detection threshold, the overall sensitivity of the system was increased by 15 dB. Although the improved sensitivity would have been useful in the first few days of monitoring, it was not relevant for the later stages of hydration. More than half of the total hits detected during the test were detected after increasing the system sensitivity, but none of these hits were detected on more than two channels simultaneously, and the average absolute detection energy was less than 0.1 μJ. Without the increased detection sensitivity, most of these hits would probably not have been detected.

A review of the AST data indicated that signal attenuation during the first few days of hydration was very high, which was corroborated by relatively poor detection sensitivity during the first two pencil break tests. Due to a lack of usable AST data until the final 10 days of the test (after recovery from a computer shutdown), attempts to measure changes in ultrasonic velocity and attenuation throughout the hydration process failed. These values must be measured using an alternative approach before conducting the next AE test of a specimen developed using appreciable volumes of grout. If the majority of cracking events are determined to occur within the first few days of hydration, then the severity of signal attenuation may require a revision to the AE monitoring approach.

In the absence of significant natural acoustic events within the grout, the artificial events produced by pencil lead breaks provided most of the performance data from this test. Representative signal characteristics and qualitative performance evaluations for the four pencil lead break tests performed during test are included in Table 3-7. For comparison, data from the burst sequence signals (event C) are included.

As testing progressed, pencil lead breaks were detected both with greater reliability and by more channels simultaneously. The frequency content and energy levels of detected signals also increased as the test progressed. These trends indicate that attenuation diminished as the grout hardened. Event location during the first 10 days of testing were poor, most likely due to insufficient numbers of hits associated with each acoustic event and because the ultrasonic velocity in the grout was significantly different than the assumed velocity. Note that the test plan had assumed that the correct velocity data would be captured from the AST data.

During the final week of the test, the grout exhibited the anticipated L-wave speeds. All pencil breaks in the final pencil break test were detected, and most pencil breaks were detected by every AE sensor channel. Due to the orientation of the lead breaks on the grout top surface, the compression wave tended to favor downward propagation, and the AE channel located at the bottom center of the test stand (CH16) tended to detect the events at much higher energy levels than the other channels. Location accuracy also improved by the end of the test. Part of the pencil break test involved a “line break test” to check location accuracy. During this test, 13 pencil breaks were performed at the top center of the specimen, and then 3 additional breaks were performed in 25 mm [1 in] increments from the center toward CH09 (Figure 3-12). The pencil break locations are represented as 13 green squares. The calculated AE event locations are color coded by amplitude response in dB_{AE}.

In the *XZ*-plane only, events were detected with an average location error of 11.6 mm [0.46 in] and a standard deviation of 10.7 mm [0.42 in]. When the volumetric location accuracy was considered, the location error increased to 60.3 mm [2.4 in] with a standard deviation of 33.3 mm [1.3 in], due largely to a systematic depth error. A significant part of the depth error was produced by a limitation of the location algorithm. The algorithm employed had difficulty accurately locating events that were found outside of the volume enclosed by the sensor grid, and tended to find the nearest match within the grid volume. A large fraction of the AE events were aligned with the top row of sensors. This limitation may be corrected in future experiments by modifying the sensor arrangement and adjusting how the algorithm handles preliminary event locations found near sensor boundaries.

Table 3-7. Representative Signal Characteristics of Pencil Lead Break Tests

Event Label* and Date	Average Amplitude Response (dB_{AE})	Average Detected Energy (µJ)	Average Centroid Frequency (kHz)	Average Peak Frequency (kHz)	Detection Likelihood	Location Accuracy
C (04-12-15)	59	0.14	70	18	N/A	N/A
B (04-11-15)	61	1.78	32	7	Poor	Very Poor
D (04-16-15)	68	10.83	29	5	Poor	Poor
E (04-20-15)	64	18.29	126	98	Moderate	Moderate
H (05-12-15)	76	531.42	142	112	High	Moderate

*Event labels are the same as given in Figure 3-10 and Table 3-6.

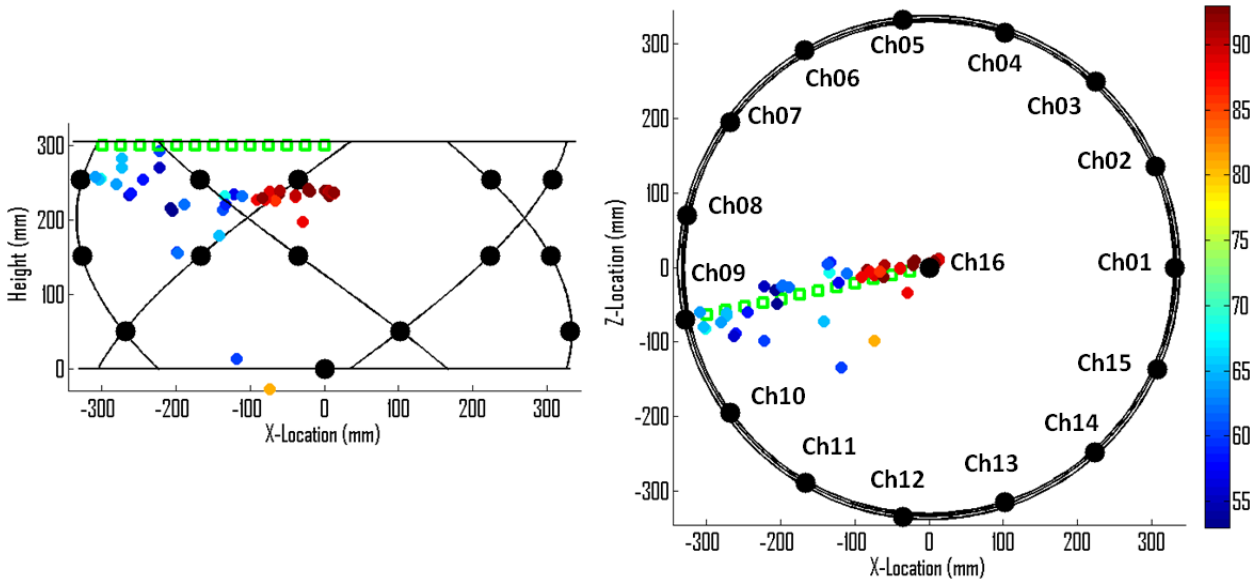

Figure 3-12. AE Event Locations for 39 Pencil Lead Breaks Performed in Sets of 3 Along 13 Locations in a Line Between the Top Center of the Specimen and CH09. Located Events are Color Coded by Maximum Signal Response in dB.

3.3.4 Summary of Preliminary Mesoscale AE Monitoring Experiment

Based on the monitoring data, the SRS reducing tank grout specimen is assumed to be either free of significant cracks, or else cracks formed during an early stage when severe signal attenuation in the gel-like grout prevented reliable signal detection. Past experience suggests that cracking was not generally observed in mesoscale grout specimens, so one might not expect to have observed early cracking during this mesoscale AE experiment due to its relatively small size. If any macrocracking events occurred within the first one to three days following grout placement, they went undetected. Measurements of the background acoustic activity of this specimen also indicated that the tank grout produces only minimal spurious signals, the majority of which were confined to a narrow time window between 33 and 47 hrs after grout placement. This indicates that minimal data filtering will be required to sort cracking events from unrelated data in the AE monitoring scheme.

Due to the severity of signal attenuation early in the grout hydration process, attempts to use ASTs to measure changes in ultrasonic velocity and attenuation throughout the process failed. If the majority of cracking events are determined to occur within the first few days of hydration, then the severity of the signal attenuation may require a revision to the AE monitoring approach. Some improvements were made to the acquisition settings over the course of this experiment, but additional improvements will be required to overcome the level of attenuation observed during the early stages of hydration. Revisions to the AE monitoring technique will be considered prior to proceeding to the next mesoscale AE tank grout monitoring experiment.

Once the mesoscale specimen had begun to harden, the AE system began to reliably detect and locate artificial crack signals produced by pencil breaks. By the end of the test, the system was demonstrating 100 percent detection of pencil lead breaks and could locate the majority of the breaks on the top surface of the grout with passable accuracy. In hardened grout, the greatest contributor to location error appears to be a logical limitation in the location algorithm. This limitation can be partially addressed by modifying sensor configuration and logical settings

in the AE system. At this time, sufficient velocity data is not available to reliably locate signal sources in the grout in its early stages of hydration. An alternative experiment described in Section 3.4 was devised to capture this information.

3.4 WAVE DISPERSION AND ATTENUATION MEASUREMENTS OF HYDRATING SRS REDUCING TANK GROUT

As discussed in Section 3.1, the velocity and attenuation of acoustic waves propagating in grout vary over wide ranges during the hydration process. Experiments were performed to measure the final acoustic parameter values for both longitudinal and shear waves on hydrated specimens, so the final values for velocity and attenuation are well understood. The early stage values for velocity and attenuation, however, were not known and no appropriate values were available in the literature. Without this information, accurate identification of AE events that occur in the hydrating grout would not be possible. Thus, an experiment was performed to measure the acoustic velocity and attenuation information in the hydrating grout. This section describes the experimental approach, data analysis technique, and the results from this test.

3.4.1 Experimental Approach

An ultrasonic through-transmission experiment similar to the setup described by Aggelis et al. (2005) was designed to measure the L-wave phase velocity and attenuation during the hydration and hardening of SRS reducing tank grout, where group velocity is computed from the phase velocity information. Two Panametrics V413 transducers {500 kHz center frequency, 13 mm × 25 mm [0.5 in × 1 in]} were mounted within cavities machined into rectangular acrylic plates (Figure 3-13). The two plates were bolted together with machined metal standoffs to control the separation between the two transducers, and closed-cell foam material combined with vacuum grease were compressed between the two plates to form a cavity for the tank grout. Once the cavity was filled with fresh grout, ultrasonic waves were transmitted through the grout. Data were collected at multiple frequencies, and this information was used to quantify wave propagation time through the material and the amplitude of the received signals.

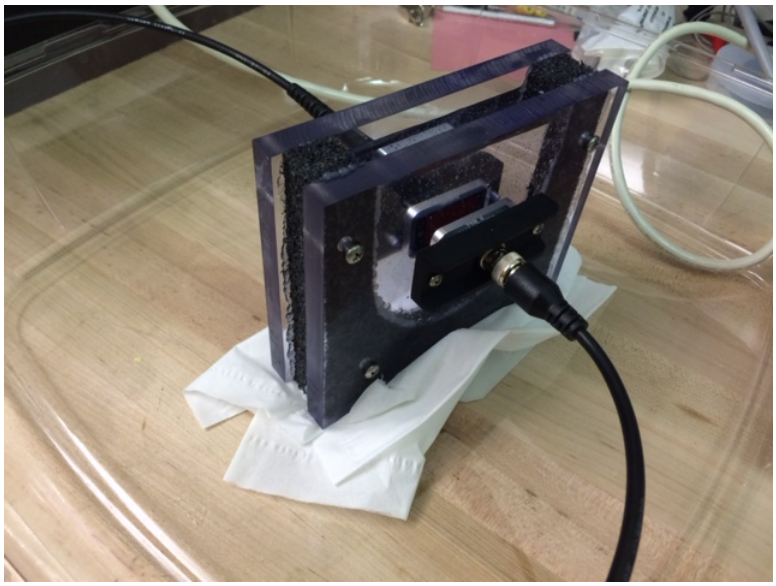

Figure 3-13. Phase Velocity and Attenuation Measurement Test Fixture

An automated data acquisition system was assembled using available laboratory equipment to periodically collect waveforms at multiple frequencies throughout the initial hydration process. Measurements are performed at multiple frequencies because the acoustic parameters are not constant across all frequencies. A functional block diagram showing key components for the acquisition system is shown in Figure 3-14. A laptop running a custom acquisition program developed using National Instruments (NI) Labview controlled the system. Periodically, the software triggered an Agilent 33220A function generator to produce 5 V_{pp}, 10-cycle tone bursts, incrementing in 10 kHz intervals from 50 to 250 kHz. Multiple waveforms were collected at each frequency to facilitate signal averaging. The function generator drove the transmitter probe, and the propagating wave was detected by the receiver probe. The received signal was amplified by a fixed gain, ranging from 0 to 60 dB, using a Panametrics 5073PR pulser/receiver. A Krohn-Hite 3900 low-pass filter was applied to the signal with a cutoff frequency of 400 kHz to prevent aliasing. Finally, the signal was digitized by an NI CompactRIO (cRIO) at 1 megasample/second. Once each waveform was captured in memory, the cRIO would transfer the data to the laptop for storage and later evaluation.

Data collection began immediately after freshly mixed grout was poured into the cavity formed by the acrylic plates and closed-cell foam. Each acquisition cycle lasted approximately 20 minutes, during which a total of 420 waveforms were collected (20 waveforms at each of 21 test frequencies). After each acquisition cycle, the acquisition system went to idle state for 30 minutes before capturing the next data set. The data collection process was allowed to run uninterrupted for several days. The signal levels varied dramatically during the test, which required the test operator to adjust the gain at least daily to protect against signal saturation.

Following acquisition of a data set, the system software was commanded to wait 30 min before restarting this process. The data collection process was allowed to run uninterrupted for several days but data were only used from the first three days because the acoustic parameter values appeared to reach steady-state prior to this point.

A total of three tests were performed using this experimental setup. The first test performed used an 18.9 mm [0.743 in] separation between the acrylic plates. This test lasted approximately 7 days, but meaningful data were collected only during the first 3 days. After approximately 3 full days of data collection, the grout pulled away from one or both acrylic surfaces which produced a sudden and dramatic decrease in signal amplitudes. The second test used a 25.3 mm [0.994 in] separation between the acrylic plates. This test lasted approximately 7 days with no issues discovered during the testing. The third and final test was conducted with water instead of grout at the 25.3 mm [0.994 in] separation configuration. Only one waveform was collected for each of the test frequencies and a single set of waveforms were collected (i.e., 21 total waveforms). This test was used as a reference for the attenuation measurements.

3.4.2 Data Analysis

The data were analyzed in the Mathworks MATLAB® development environment on a computer workstation. Prior to performing the analysis to determine the velocity or attenuation, all of the data recorded by the test system were preprocessed to improve the signal quality. This step included high pass filtering the waveforms to remove any frequency components below 30 kHz, averaging all 20 waveforms collected at a single frequency for each acquisition cycle (for the grout data tests), compensating for any variations in instrumentation gain, and upsampling the data from 1 megasample per second to 10 megasamples per second. Additionally, waveforms

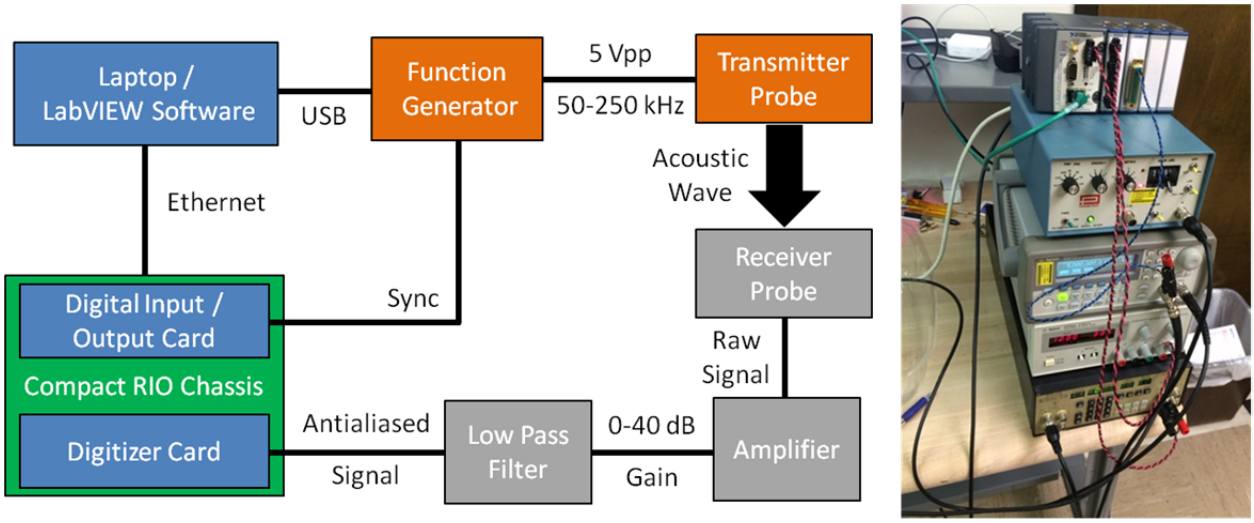

Figure 3-14. Functional Block Diagram Showing Signal Paths in Experimental Approach (Left) and Laboratory Electronics Used With Ultrasonic Setup (Right)

whose received signals were identified as saturated were removed from the dataset. Signal saturation was a major issue that is discussed in Section 3.4.3.

After preprocessing, the data were processed to either measure the attenuation or phase velocity. The process for computing the signal attenuation was to compare the data collected from the hydrating grout specimen with the data collected from water in the test fixture, where all data were collected with a 25.3 mm [1 in] separation between the inner surfaces of the fixture. Two requirements were imposed on the data prior to calculating the attenuation:

a) neither grout nor water reference signals were collected with saturated receivers, and

b) both signals have at least 20 dB signal-to-noise ratios (SNR) for transmitted acoustic waves through their respective material.

If both requirements were met, attenuation was computed by windowing around the largest amplitude in the signal with a Hanning window and transforming the signals to the frequency domain using a fast Fourier transform algorithm. The peak amplitude was measured in the transformed data (i.e., in the frequency domain) at the same frequency used during data generation. The attenuation relative to water was then computed for each test frequency *(f)* and time *(t)* post-placement with the following algorithm:

$$Attenuation\ (f,t) = -\frac{20}{x} log_{10}\left(\frac{A(f,t)}{A_W(f)}\right),$$

where *x* is the propagation distance through the grout or water [25.3 mm (1 in)], $A(f,t)$ is the amplitude measured in the grout at each frequency and time point, and $A_W(f)$ is the amplitude measured at each frequency in water.

Phase velocity was computed using the data collected via the two acrylic plate separation distances {18.9 and 25.3 mm [0.75 and 1 in]}. The same two sample requirements were

imposed on the data, namely 20 dB SNR and no receiver saturation, before processing it at a given frequency and time. Assuming these two conditions were met, the phase velocity was computed using the time domain signals directly. The process was as follows:

1. Identify the time of largest amplitude peak in the 18.9 mm [0.75 in] configuration signal.

2. Find the first negative-going zero crossing after this peak time in the 18.9 mm [0.75 in] configuration signal.

3. Find the first negative-going zero crossing in the 25.3 mm [1 in] configuration signal that occurs after the time index identified in Step 1.

4. Compute the phase velocity as the propagation distance difference (6.4) divided by the time difference between zero-crossings (Steps 2 and 3).

This process makes two important assumptions. First, it assumes that the phase velocity is strictly positive, which is reasonable for most materials. Second, it assumes that the first negative going zero-crossing in the 25.3 mm [1 in] configuration occurs after the same signal phase identified in the 18.9 mm [0.75 in] signal. To ensure that this assumption was reasonable, a large number of signal sets were visually examined to ensure that this assumption was reasonable with no problems identified.

3.4.3 Attenuation Results

The overall attenuation results are shown in Figure 3-15. For the attenuation results, the peak measured attenuation was approximately 2 dB/mm [50 dB/in]. Using the existing equipment setup, it was not possible to generate sufficient signal amplitude to measure greater attenuation levels, so instances of even higher attenuation were not calculated. This is observed as a large red region that spans the upper portion of Figure 3-15. After the first day, attenuation decreased significantly and settled to nominally steady-state values during the second day. An example attenuation over time curve for the 140 kHz frequency data is shown in Figure 3-16, where attenuation appears to reach a steady-state value of 0.77 dB/mm [19 dB/in] after 2.2 days.

Two large white regions are also observed in Figure 3-15 in the 50–75 kHz range and the 100–130 kHz range. These regions correspond to instances where recorded signals became saturated. Across the 70 data sets collected in the first 2.4 days at all 21 frequencies, a total of 144 measured waveforms were saturated and therefore not useable (out of 1,470 waveforms). These two regions likely correspond to relatively low attenuation. Throughout testing, the fixed gain had been adjusted based on the signal response at 250 kHz. Less attenuation was anticipated at lower frequencies, but actual amplitude variation across the frequency range during each acquisition cycle was larger than anticipated. If attenuation is needed for these unmeasured regions, the experiment would need to be repeated or redesigned to compensate for the large dynamic range of the signals as a function of frequency.

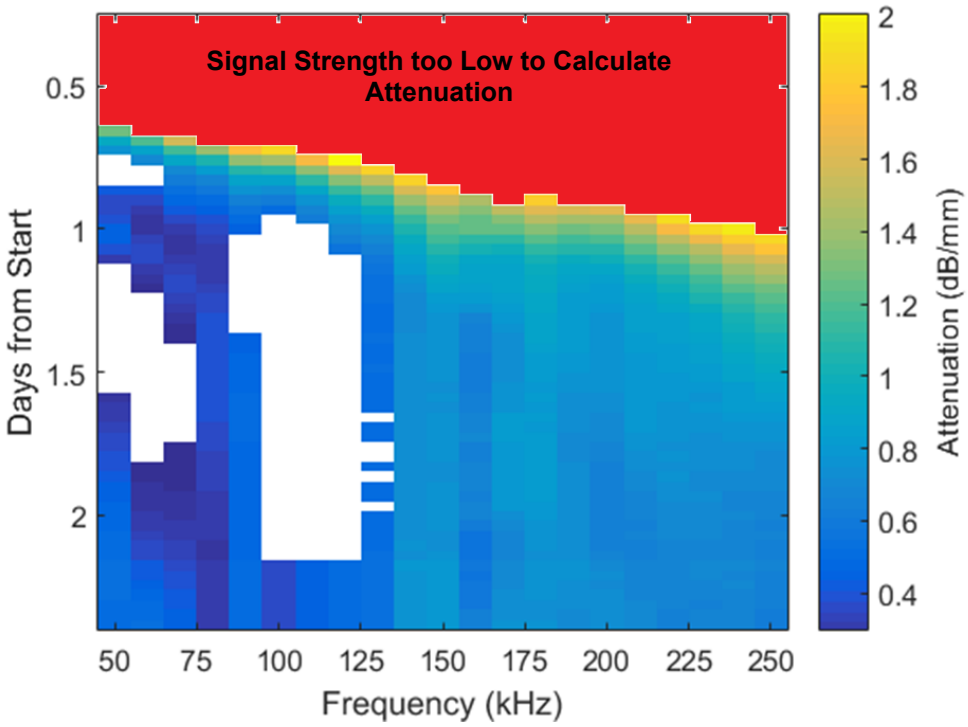

Figure 3-15. Measured Overall Attenuation Relative to Water

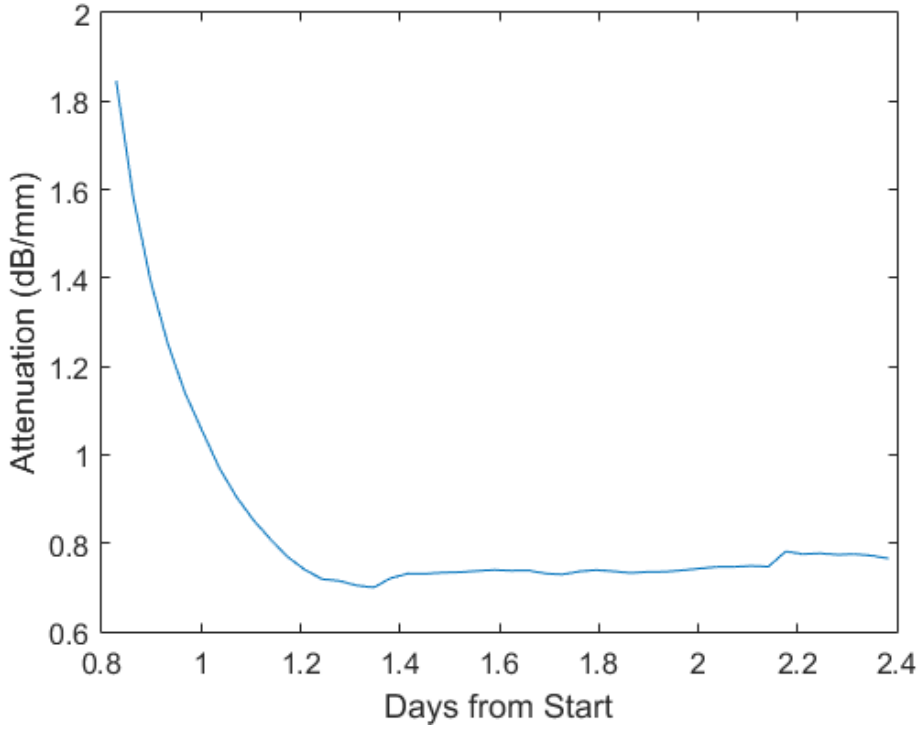

Figure 3-16. Measured Attenuation for the 140 kHz Input Frequency Signal as a Function of Time From Experiment Start

Although the attenuation profile shown in Figure 3-15 is consistent with values found in the literature for similar materials (Aggelis, 2005), it is not consistent with the measured attenuation discussed in Table 3-2 or the AE results discussed in Table 3-6. In Table 3-2, the attenuation in fully hydrated grout was measured as approximately 0.06–0.08 dB/mm [1.5–2.0 dB/in]. Furthermore, if attenuation values comparable to those shown in Figure 3-15 had been observed in the AE experiment to monitor hydrating SRS reducing tank grout, then it is highly unlikely that pencil break tests performed throughout the monitoring period would have registered as detectable events. One of the major differences between the two attenuation measurement approaches is that in Section 3.1, attenuation was measured using two different grout specimens with two different thicknesses, but in this experiment, attenuation was measured relative to water in place of the grout. It was decided to test whether this difference in approach would result in substantially different results by using the amplitude information available from the two different hydrating grout experiments. The analysis equation for computing attenuation was updated as shown here:

$$Attenuation\ (f,t) = -\frac{20}{s} log_{10}\left(\frac{A_{large}(f,t)}{A_{small}(f,t)}\right)$$

where the subscript of the amplitude variable, *A*, denotes if it was from the large or small separation distance between the acrylic plates and *s* is the difference in the two separation distances. The result of this calculation is shown in Figure 3-17. Note that as in Figure 3-15, Figure 3-17 includes a red region that signifies points where attenuation was too great to measure and two white regions where signals became saturated and could not be used for attenuation calculation. Using this method, both very large and very small attenuation values are present, and negative attenuation values are present, as well. Instances of negative attenuation correspond to time-frequency points that produced greater signal amplitude responses at the longer wave path than at the corresponding shorter wave path. Presently, there are two hypotheses for the occurrence of negative attenuation values. First, given the relative size of the aggregate compared to the size of the separation between the acrylic plates, there is potential for high variability in the packing factor of the aggregate within the wave path between the two transducers. If in one setup the aggregate fills a substantial portion of the propagation path whereas in the other setup the path is dominated by cementitious material, then large variation in results could occur. Second, if the attenuation levels are in agreement with the values reported in Section 3.1, the total attenuation for a reverberation between the acrylic plates would be on the order of 4 dB per reverberation. This could potentially cause issues where phases bouncing between the acrylic plates destructively or constructively interfere with the later phases. Given these challenges in the measurement approach, the attenuation values reported in this section are not considered reliable and the measurement approach must be revised to support AE monitoring.

3.4.4 Phase Velocity Results

The overall phase velocity measurement results are shown in Figure 3-18. Note that causes of the amplitude variations discussed for the attenuation measurements should not grossly affect the results of this analysis. As with the attenuation measurements, there was insufficient signal amplitude to perform the analysis during the initial experiment stages, denoted by the red region at the top of the figure. After the first day of setting, the phase velocity appears to slowly increase from a value of approximately 2 mm/μs to a steady-state value. For example, Figure 3-19 shows the phase velocity versus time curve for the 140 kHz test frequency. For this example, the phase velocity steady state value approaches 5.5 mm/μs. There are also regions

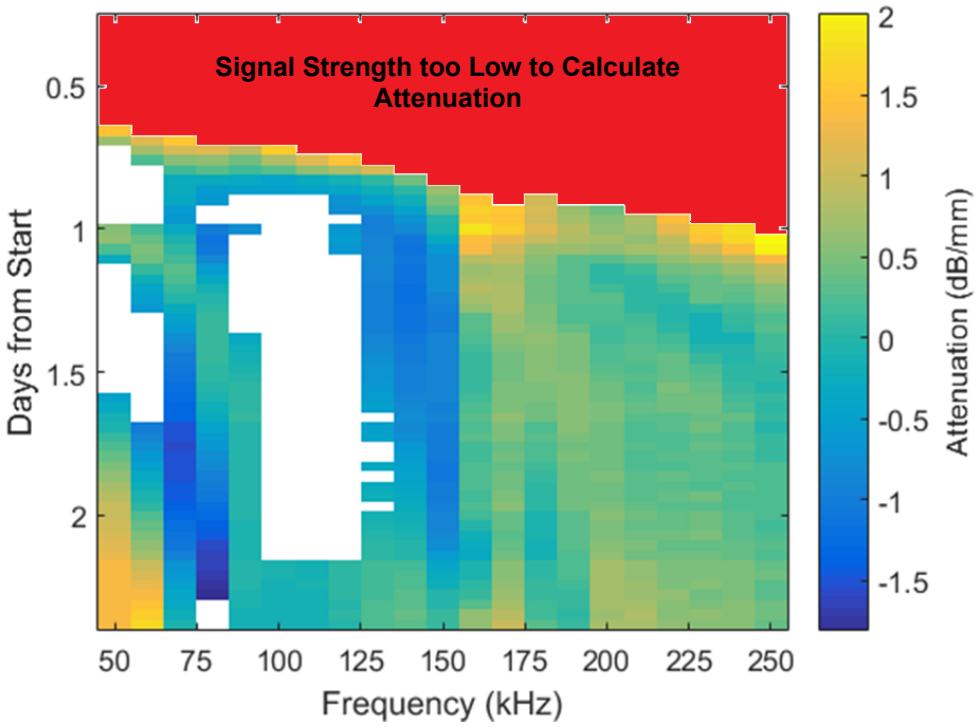

Figure 3-17. Measured Overall Attenuation Using Two Grout Thicknesses for the Calculation

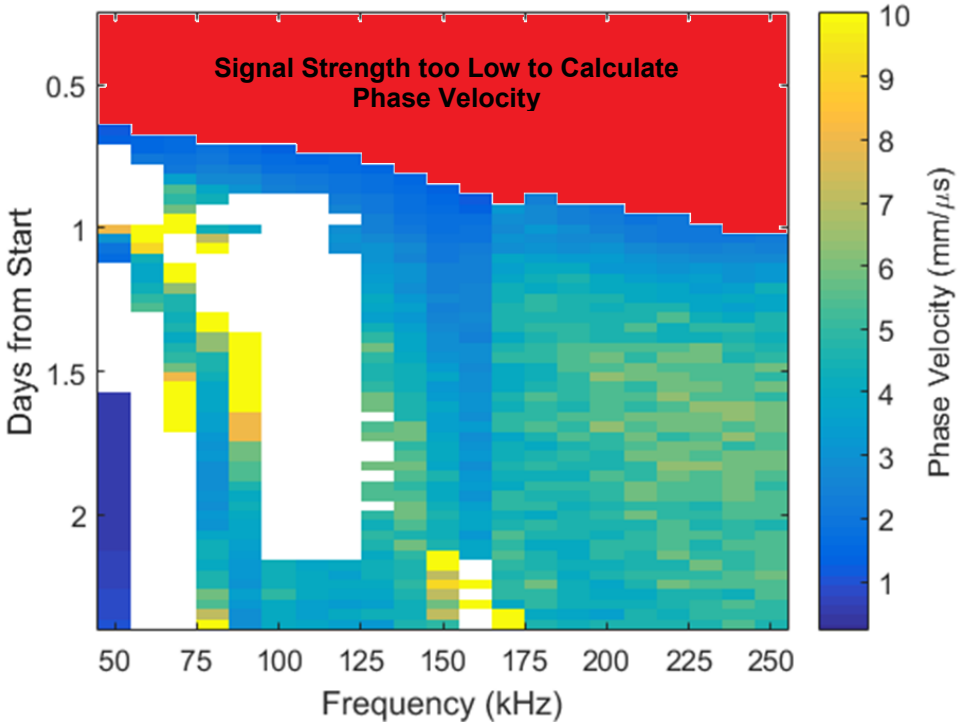

Figure 3-18. Measured Overall Phase Velocity

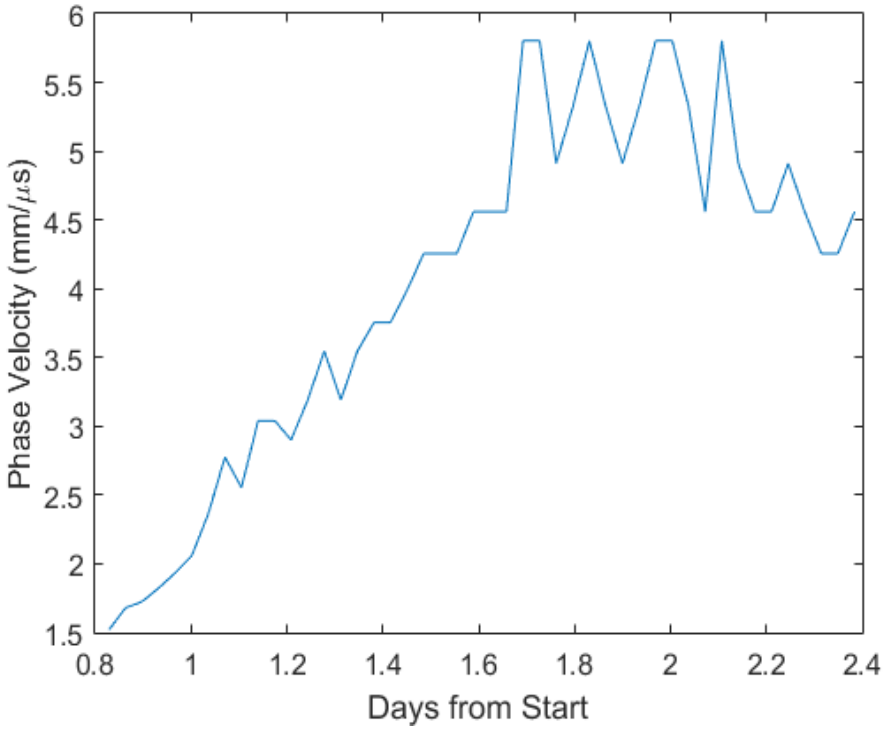

Figure 3-19. Measured Phase Velocity for the 140 kHz Input Frequency Signal as a Function of Time From Experiment Start

where the phase velocity was very high (>10 mm/μs). While not initially expected, similar results were reported when testing mortar using a similar experiment (Aggelis, 2005).

As with the attenuation measurements, there are large regions where the phase velocity was not measurable due to signal saturation of the receiver electronics. Group velocity, which is ultimately what is needed by the AE system, is related to the phase velocity using the following equation:

$$C_{group} = C_{phase}\left(1 - \frac{\omega}{c_{phase}}\frac{\delta c_{phase}\,(f,t)}{\delta\omega}\right)^{-1}$$

In this equation, C_{phase} is the phase velocity, C_{group} is the group velocity, and $\boldsymbol{\omega}$ is the angular frequency. From this relationship, it is necessary to compute the change in phase velocity as a function of frequency, and this would not be possible in these regions where the data are not continuous. Unfortunately, this region where data are not available is also where the signal attenuation is the lowest. Thus, any signals received by the AE sensors would likely have frequency content centered on this low-attenuation region, but the group velocity in this region is unknown. Given this error, a repeat of this experiment is necessary to correct for experimental errors. Additionally, since the attenuation results are considered suspect, it may prove better to redesign the overall experiment to allow more accurate measurement of attenuation as well as direct measurement of the group velocity instead of relying on conversion from the phase velocity.

4. SUMMARY AND CONCLUSIONS

The Center for Nuclear Waste Regulatory Analyses (CNWRA®) conducted a sequence of active ultrasonic and acoustic emission (AE) experiments on specimens of tank grout and saltstone to evaluate the feasibility of using AE technology for passively monitoring crack formation within cementitious tank grout and saltstone, including during the early stages of hydration when the cementitious materials are in a gel form and challenging to monitor acoustically. CNWRA staff had previously noted that certain cracks formed during the first 24 hrs after grout placement in the intermediate-scale grout monolith, which provided motivation for including the earliest stages of grout and saltstone evolution in the monitoring process. These experiments were designed to explore whether AE sensors encapsulated within grout during grouting operations could passively monitor waste tank grout and saltstone monoliths for crack formation, record the timing and location of cracking, and map crack propagation. The timing and location information would be useful in diagnosing the mechanisms of crack formation. The primary objectives for this feasibility study were to develop an AE monitoring technique to identify the timing and location of cracks that form within a grout monolith using commercially available AE equipment and to verify the technique on mesoscale test specimens. In addition, the following secondary objectives were considered:

- Measure ultrasonic properties in fresh and fully hydrated grout
- Optimize the monitoring sensor configuration, instrumentation, and acquisition settings for the given materials and specimen geometry
- Characterize background signal sources produced by the hydration process
- Characterize propagating wave modes and changes in speed during initial stages of hydration and setting

A sequence of experiments was conducted to determine the ultrasonic properties of the two types of materials, develop an AE monitoring technique capable of detecting and locating cracking events in the two types of materials, and evaluate the monitoring technique on mesoscale specimens. Ultrasonic experiments were performed using standard ultrasonic probes and driver instrumentation. The AE experiments were performed using a 16-channel Physical Acoustics Corporation DiSP Acoustic Emission Workstation, Model PCI–2 (AE instrument), which was provided to the team for its use by Southwest Research Institute® Geosciences and Engineering Division.

4.1 ULTRASONIC PROPERTIES OF HARDENED GROUT

The initial experiment focused on measuring the basic ultrasonic properties of both materials in their hardened state. Specimens of tank grout and saltstone were destructively tested using an ultrasonic through-transmission technique to accurately measure the longitudinal wave and shear wave speeds and estimate the ultrasonic attenuation in each material. Tests performed in both materials indicated that wave propagation was preferential to the 100–150 kHz frequency band, but relevant ultrasonic information may be present at frequencies as high as 400 kHz. For tank grout, the longitudinal (L-wave) speed, shear (S-wave) speed, and attenuation were determined to be 4.14 ± 0.26 mm/μs, approximately 2.9 mm/μs, and 65–75 dB/m [20–23 dB/ft] at 130 kHz. The velocity measurements have been determined to be valid through other ultrasonic and AE experiments performed throughout the fiscal year.

Further verification of the attenuation estimate may still be needed. Testing of a saltstone specimen that was allowed to harden under high humidity and ambient temperature conditions yielded measurements of 2.39 mm/µs, 1.13 mm/µs, and 80–100 dB/m [24–30 dB/ft] for L-wave speed, S-wave speed, and attenuation. To date, testing of various saltstone specimens has indicated that the ultrasonic properties of saltstone are highly dependent on the environmental conditions during hydration, so the nominal ultrasonic properties have not been determined with certainty. Property testing of saltstone may need to be revisited once new laboratory control procedures for hydration of specimens have been established.

In both tank grout and saltstone, waveforms transmitted in the S-wave mode exhibited very poor amplitude response compared to waveforms transmitted in the L-wave mode, but both modes appeared to exhibit comparable rates of attenuation. Based on the relative signal responses, both tank grout and hydrated saltstone appear to be poor conductors of the S-wave mode. Based on the poor S-wave signal response, it is unlikely that shear waves will be detected during AE monitoring. The absence of the S-wave mode will simplify AE monitoring by eliminating the need to separate S- and L-waves for event detection.

4.2 DEVELOPMENT AND OPTIMIZATION OF AE MONITORING APPROACH

Once basic ultrasonic property data were known from fully hydrated tank grout and saltstone, AE testing began on small, bench-top specimens of the Savannah River Site reducing tank grout and proxy saltstone to establish preliminary guidelines for AE acquisition settings, sensor arrangement, and data processing logic. Investigations were conducted by installing various configurations of AE sensors on the specimens and then performing pencil lead breaks around their surfaces. The artificial acoustic sources produced by the pencil lead breaks were used to adjust the AE instrumentation settings. Information regarding the timing and location of the pencil breaks was used to tune an event location algorithm and evaluate the detection sensitivity and location accuracy of various sensor configurations applied to the specimens. Using this evaluation technique, an AE sensor configuration and corresponding instrumentation settings were selected for further development on larger test specimens. The sensor configuration consisted of three bands of 5 sensors mounted near the base, at the midline, and near the top of the cylindrical specimen. The sensors were staggered by 72° in each band, and each band led the preceding band by 24°. Viewed from overhead, the configuration consisted of 15 AE sensors clocked at 24° intervals about the circumference of the specimen. A 16th sensor was located at the bottom center of the specimen. Using this configuration and the selected instrumentation settings, event location was typically accurate to within 20 mm [0.8 in], which corresponds to a distance of one wavelength at the typical propagating wavelengths in the specimens.

Concurrent with the ultrasonic property tests and the AE technique development, CNWRA had begun preparations for an experiment where a 108 L [28.5 gal] specimen of tank grout would be AE monitored from initial placement through the first full month of hydration and hardening. Among the various objectives of this test was the goal of evaluating and refining the AE monitoring technique initially developed on the small, fully hydrated bench-scale grout specimens. For this test, the AE sensor configuration was rescaled to accommodate the increased volume of the specimen, and the acquisition and instrumentation settings were adjusted accordingly. Over a period of 32 days of monitoring, the collected data provided sufficient information to make improvements to the waveform timing capture logic and adjustments to the detection threshold, leading to an overall system sensitivity increase by 15 dB and to general improvements to the capability of the system to capture AE events. Throughout the test, no naturally occurring AE events were detected, and the specimen was

assumed to harden without the formation of any significant cracks. In the absence of significant natural acoustic events within the grout, the artificial events produced by pencil lead breaks provided most of the performance data from the test. Because the changes in wave velocity throughout the grout hydration process had not been characterized by the conclusion of this test (which will be discussed further in a later section), event location could only be rigorously evaluated at the very late stage of hydration when wave velocity was well known. From pencil break tests performed on the top surface of the specimen, the AE monitoring system demonstrated 100 percent detection capability in the late stage of hardening and was able to locate breaks with an average error of 11.6 ± 10.7 mm [0.46 ± 0.42 in], provided event location was confined to the top surface. When volumetric location was considered, the location error increased to 60.3 ± 33.3 mm [2.37 ± 1.31 in]. The increase in error was due largely to a systematic depth error produced by a known limitation in the implementation of the location algorithm. The algorithm had difficulty accurately locating events that occurred outside of the volume enclosed by the sensor grid. In this test, the algorithm attempted to produce location results that were in plane with the uppermost band of AE sensors, which produced a systematic depth error. This limitation may be corrected in future experiments by modifying the sensor arrangement and adjusting how the algorithm handles preliminary event locations found near sensor boundaries.

4.3 ACOUSTIC BACKGROUND SIGNALS PRODUCED BY HYDRATION

An important secondary goal of the experiment to AE monitor the hydration process of the mesoscale, 108 L [28.5 gal] specimen of tank grout was to record and characterize any acoustic background signals that may be produced by the hydration process. It was important to detect and characterize extraneous signals that are unrelated to cracking in small specimens of grout so that in experiments on larger specimens, the same signals can be readily identified and filtered from the data, thereby reducing the risk of falsely identifying crack signals. In the hydration experiment on the mesoscale specimen of tank grout, extraneous signals were detected only during a narrow 14-hr timespan that began 33 hrs after initial grout placement. The signals detected in this timeframe were highly repetitive, extremely low energy, and exhibited spectral characteristics that were atypical of crack signals. These signals, which were dubbed burst sequence signals due to their highly repetitive presentation, should be easily identifiable in future testing due to their unusual characteristics.

Assuming the burst sequence signals are the only extraneous signals produced by the hydration process, minimal data filtering should be required to separate background noise from relevant AE signals. It is possible that at increased AE sensitivity other background signals could be detected, but at present sensitivity levels, pencil breaks have shown that AE monitoring of tank grout is viable as early as two days after initial placement. Additional testing at greater sensitivity may be needed to ensure noise-free monitoring in the first two days after grout placement.

No monitoring was conducted of hydrating saltstone to characterize its background noise level during this reporting period.

4.4 VARIATION OF WAVE SPEED AND ATTENUATION DURING HYDRATION

Efforts to characterize changes in wave speed and attenuation throughout the grout hydration process have met with limited success so far. Two experimental approaches were attempted to capture this information. The first approach attempted to capture these data incidentally during the mesoscale AE monitoring experiment. The approach relied on periodically performing

Automated Sensor Tests (AST) measurements throughout the test. The AST data would provide velocity and signal response data through a large number of propagation paths throughout the specimen, and the signal loss data could be used to calculate attenuation. Attempts to measure velocity and attenuation change using this process failed because the severity of the attenuation in the first several days of hydration rendered the AST data unusable. Although an approximate estimate of attenuation for fully hydrated tank grout was known and the attenuation of gel-like grout was assumed to be much higher, the actual attenuation proved to be greater than expected.

A second experiment was conducted to capture the wave speed and attenuation data directly by performing periodic automated through-transmission tests on two specimens of grout with two known thicknesses and on a reference of water, using their relative signal responses and times-of-flight to calculate attenuation and phase velocity at each stage in hydration. The group velocity data could then be derived from the phase velocity data. This approach also had the added benefit of revealing any instances of velocity dispersion in the grout if frequency dispersion was present. Initial testing was performed on tank grout. Although this experiment demonstrated some moderately promising results, several experimental complications arose that diminished the value of the velocity results and undermined the validity of the attenuation results. Even given the relatively short wave propagation distances of this test, the attenuation was too great for reliable signal detection prior to roughly 20 hrs after grout placement. After the first day of hydration, attenuation diminished precipitously, causing signals to saturation in the frequency bands of greatest interest (50–75 kHz and 100–125 kHz). Reliable calculations of velocity and attenuation could not be made using saturated signals. Finally, calculation of attenuation by comparing signal responses of the two grout specimens produced instances of negative attenuation, where signal response at a given frequency and hydration state was greater through the thicker specimen than it was through the thinner one. While the cause of the negative attenuation values is not known, their presence implies variation in the material consistency that complicates calculation of attenuation using this approach.

Despite the experimental shortfalls, this experimental approach to measuring change in wave speed and attenuation did yield some promising results. The relative attenuation profile compared to water exhibited drastic reduction in attenuation 20–24 hrs after grout placement, and lowest attenuation was observed in the two frequency bands previously noted to be most conducive to AE monitoring. Although signal saturation prevented analysis of signals in these frequency bands, measurement of phase velocity appeared to be successful at higher frequencies. If the experiment were repeated, the test would be attempted with larger specimen volumes, which would reduce the effect of material variation on attenuation and allow simultaneous direct measurement of both phase velocity and group velocity. To compensate for the increased signal loss posed by a larger specimen volume, higher power probes and pulser instrumentation would be used. Finally, the acquisition procedure would be adjusted to avoid instances of signal saturation.

4.5 OVERALL STATUS OF AE MONITORING TECHNIQUE

From the ultrasonic property data and AE experimental data collected to date, it appears that the AE monitoring technique is capable of monitoring moderate volumes of tank grout for crack detection after the initial stages of hydration are complete (nominally after one week) and is capable of locating crack events with moderate accuracy once the tank grout reaches a state of full hydration. Refinements made during testing could be applied to future tests to achieve immediate detection performance improvements. The present performance limitations of the AE monitoring system result from three factors:

- High levels of attenuation in the grout during early stages of hydration
- Insufficient material property data on changes in ultrasonic speed and attenuation
- Insufficient system optimization with all factors known, including all material property information

It may be possible to reduce the effect of attenuation on detection sensitivity, but in light of the severity of attenuation during the first day of hydration, it is unlikely that the limitation of attenuation will be completely overcome. The AE detection sensitivity may be effectively increased by implementing acquisition settings that reduce the noise floor and increase signal detection range, and additional signal sensitivity may be achieved by replacing preamplifier hardware and AE probes with hardware that is more sensitive to the relevant monitoring frequency ranges in the grout materials. Even with these changes, attenuation during early hydration may act as a limiting factor on the detection capability of the system. AE monitoring of large specimens may require tradeoff between detection sensitivity and volumetric location capability. Thus, AE may be used effectively as a two-dimensional detector for crack signals over a broad range of energy levels or as a three-dimensional detector only for high-energy crack signals, but not both simultaneously.

5. RECOMMENDATIONS FOR FUTURE WORK

Additional testing is required to complete characterization of the ultrasonic properties of tank grout and saltstone. Once the remaining required property data are established, Center for Nuclear Waste Regulatory Analyses (CNWRA®) staff will be able to optimize the acoustic emission (AE) monitoring technique. Provided the technique is determined to be effective at detecting and locating cracks in mesoscale specimens of tank grout and saltstone, CNWRA staff may recommend steps to scale the AE monitoring technique for implementation at field scale. Possible tasks to develop the AE monitoring technique are listed below.

1. Conduct additional ultrasonic through-transmission tests on specimens of saltstone that are allowed to hydrate at 100 percent humidity conditions and at high ambient temperature conditions.

   Ultrasonic through-transmission measurements in various saltstone specimens indicated that the ultrasonic properties of the material are highly dependent on the environmental conditions during the hydration process. Unlike the measurements acquired from tank grout, the final velocity values from saltstone were acquired from a relatively small specimen that could not be tested with the same level of rigor and therefore did not produce the same level of confidence in the velocity measurement. Additional tests on specimens of saltstone hydrated under environmentally controlled conditions using the existing measurement procedure would be useful to verify existing values for wave speed and attenuation obtained from hardened, hydrated specimens.

2. Revise and repeat the ultrasonic phase velocity and attenuation experiment

   Despite the experimental complications encountered in the first attempt, the experiment to directly measure ultrasonic phase velocity and attenuation through grout during its hydration process produced promising results, and the experiment merits repeating to collect an improved dataset. The complications encountered in the first test can be summarized as insufficient signal strength during the first day of testing, signal saturation at critical frequencies in the remainder of the test, and inconsistencies observed in the relative amplitude responses of the tested specimens. CNWRA staff recommends revising the experiment to address these complications. The signal inconsistencies could be diminished by increasing the wave path in each test, which would reduce signal sensitivity to local grout inhomogeneity and reduce the possibility of waveform self-interference. By increasing the wave path, the overall attenuation in each test will increase. To overcome signal loss during the test, particularly during the first day of testing, the transducers and pulser equipment will be replaced with higher power models capable of driving larger amplitude waveforms. Finally, to prevent signal saturation, either an automated gain adjust must be implemented in the system or the acquisition procedure must be adjusted to prevent saturation within the critical frequency range. Testing on specimens of tank grout and saltstone is recommended.

3. Consider other implementations of the AE monitoring technology

   The current implementation of the AE monitoring system that was developed on bench-scale specimens of hydrated grout and refined on a mesoscale specimen of hydrating tank grout was developed to balance the requirements of good detection sensitivity and good volumetric location accuracy. If the U.S. Nuclear Regulatory

Commission (NRC) determines that detection sensitivity takes priority over location accuracy, then alternative sensor configurations and adjustments to the AE acquisition settings should be considered. Sensor configurations previously investigated heavily favored sensor placement around the circumference of the specimen to permit sensor recovery after testing. Other sensor configurations could be considered.

Alternatively, if NRC determines that volumetric location of cracks is of greater importance, then attempts could be made to address known limitations of the existing location algorithm to reduce location error. Modifications to the algorithm that change the way events near sensor boundaries are addressed can be tested. Also, further adjustments to the sensor configuration can be considered.

Finally, additional AE sensors and preamplifiers could be obtained that are better suited for the specific monitoring frequency ranges now known to be important for tank grout and saltstone.

4. Develop a control procedure for the preparation of saltstone specimens with consistent ultrasonic properties for future testing.

   Prior to extensive ultrasonic and AE testing on saltstone, additional procedure development may be required to ensure that specimens produced for ultrasonic property measurement remain consistent regardless of dimensions or total volume. This may be particularly important for testing of the mesoscale specimen, where the volume is likely to exceed 100 L [26 gal].

5. Refine and repeat the experiment to AE monitor the hydration process of the 108 L [28.5 gal] specimen of tank grout. If successful, repeat the experiment for saltstone.

   Based on the lessons learned from prior experiments and the final set of ultrasonic properties for tank grout and saltstone, CNRWA staff will develop a revised test plan to AE monitor a mesoscale specimen of grout through its hydration process. Depending on the final outcome of all property data, significant revisions may be considered to the test stand to redefine the aspect ratio of specimen height to diameter or to accommodate a different AE sensor configuration. The revised test may also include supplemental sensors such as a thermocouple array to monitor the grout hydration behavior throughout testing.

   Assuming the experiment is repeated after completion of ultrasonic property testing and after re-evaluation of the AE monitoring technique, CNWRA staff anticipates conducting this experiment to confirm and demonstrate the effectiveness of the AE monitoring technique as opposed to the first test, which served largely to measure material properties and basic system performance data. CNWRA staff will repeat the test using a similar specimen of tank grout. Assuming the tank grout test is successful, the experiment will be repeated on a specimen of saltstone.

6. REFERENCES

Abeele, K.V.D., W. Desandeleer, G. De Shutter, and M. Wevers. "Active and Passive Monitoring of the Early Hydration Process in Concrete Using Linear and Nonlinear Acoustics." *Cement and Concrete Research*. Vol. 39. pp. 426–432. 2009.

Aggelis, D.G., D. Polyzos, and T.P. Philippidis. "Wave Dispersion and Attenuation in Fresh Mortar: Theoretical Predictions Vs. Experimental Results." *Journal of Mechanics and Physics of Solids.* Vol. 53. pp. 857–883. 2005.

ASTM E976–10. 'Standard Guide for Determining the Reproducibility of Acoustic Emission Sensor Response.' West Conshohocken, Pennsylvania: ASTM International. 2010. www.astm.org.

Chotard T.J., A. Smith, D. Rotureau, D. Fargeot, and C. Gault. "Acoustic Emission Characterisation of Calcium Aluminate Cement Hydration at an Early Age." *Journal of the European Ceramic Society*. Vol. 23.3. pp. 387–398. 2003.

Kaplan, D.I., K. Roberts, J. Coates, M. Siegfried, and S. Serkiz. "Saltstone and Concrete Interactions with Radionuclides: Sorption (*Kd*), Desorption, and Reduction Capacity Measurements." SRNS–STI–2008–00045. Aiken, South Carolina: Savannah River National Laboratory. 2008.

Langton, C.A. and J.R. Cook. "Recent Progress in DOE Waste Tank Closure." Waste Management Symposium 2008. February 24–28, 2008. Phoenix, Arizona. WSRC–STI–2007–00686. Aiken, South Carolina: Washington Savannah River Company. 2008.

Langton, C.A., A. Ganguly, C.A. Bookhammer, M. Koval, and W.L. Mhyre. "Grout Formulations and Properties for Tank Farm Closure (U)." WSRC–STI–2007–00641. Rev. 0. Aiken, South Carolina: Washington Savannah River Company. 2007.

Lura, P., J. Couch, O. Mejlhede, and J. Weiss. "Early-Age Acoustic Emission Measurements in Hydrating Cement Paste: Evidence for Cavitation during Solidification due to Self-Desiccation." *Cement and Concrete Research*. Vol. 29. pp. 861–867. 2009.

McLaskey, G.C., S.D. Glaser, and C.U Grosse. "Integrating Broad-Band High-Fidelity Acoustic Emission Sensors and Array Processing to Study Drying Shrinkage Cracking in Concrete." Proc. of SPIE Vol. 6529. 2007.

Pabalan, R.T., G.W. Alexander, D.J. Waiting, and C.S. Barr. "Experimental Study of Contaminant Release from Reducing Grout." *EPJ Web of Conferences*. Vol. 56. 01010. 2013. (Published by EDP Sciences).

Seaman, J.C., H.-S. Chang, and S. Buettner. "Chemical and Physical Properties of Saltstone as Impacted by Curing Duration." Savannah River Ecology Laboratory. SREL Doc.: R–14–0006. Ver. 1.0. Sept. 23, 2014.

Stefanko, D.B. and C.A. Langton. "Tanks 18 and 19–F Structural Flowable Grout Fill Material Evaluation and Recommendations." SRNL–STI–2011–00551. Rev. 1. Aiken, South Carolina: Savannah River National Laboratory. April 2013.

SRR–CWDA–2013–00026. “Requested Pre-Visit Information in Support of U.S. Nuclear Regulatory Commission F-Tank Farm March 2014 Onsite Observation Visit.” Rev. 0. Attachment 1 and 2: Grout Operations Videos; Attachment 3: Batch Tickets. March 13, 2014.

Walter, G.R., C.L. Dinwiddie, D. Bannon, J. Frels, and G. Bird. “Intermediate Scale Grout Monolith and Additional Mesoscale Grout Monolith Experiments: Results and Recommendations (Status Report).” Deliverable 14003.01.007.445. San Antonio, Texas: Center for Nuclear Waste Regulatory Analyses. September 2010.